Mesenchymal Stromal Cells Immunosuppress Osteoarthritis Synovial Fluid Tolerized Monocytes via IL-6

Condensed Title – MSC Modulate OA Synovial Fluid Tolerized Monocytes

Mozhgan Rasti[1,2], Aida Feiz Barazandeh[1,2], Kevin P. Robb[1,2,3], Rachel Low [1,2], Rajiv Gandhi[1,4], Sowmya Viswanathan*[1,2,3,5]

[1]Schroeder Arthritis Institute, University Health Network, Toronto, Ontario, M5T 0S8, Canada
[2]Krembil Research Institute, University Health Network, Toronto, Ontario, M5T 0S8, Canada
[3]Institute of Biomedical Engineering, University of Toronto; Toronto, Ontario, M5S 3G9, Canada

[4]Department of Surgery, Division of Orthopedic Surgery, University of Toronto, Toronto, Ontario, M5T 1P5, Canada
[5]Department of Medicine, University of Toronto, Toronto, Ontario, M5S 3H2, Canada

***Correspondence:**
Sowmya Viswanathan, PhD
Email: sowmya.viswanathan@uhn.ca

Abstract

The mechanisms of mesenchymal stromal cell (MSC) interactions with monocytes/macrophages (MΦs) in knee osteoarthritis (KOA) are not fully understood. We report that synovial fluid (SF) MΦs are tolerized. Healthy and OA patient donor-derived peripheral $CD14^+$ monocytes exposed to late-stage OA SF are semi-tolerized with stable phenotype, including CD86 expression with additional lipopolysaccharide (LPS) re-challenge; there were slight differences in healthy vs. OA $CD14^+$ monocyte tolerization profiles, indicative of systemic differences. Notably, both healthy and OA $CD14^+$ monocytes demonstrated non-significant or significant increases respectively in tumor necrosis factor (TNF), suggestive of an activated profile. Late-OA SF is a complex mixture of multiple factors resulting in a mixed immunosuppressed, activated, tolerized profile of $CD14^+$ peripheral monocytes. We explored the in-depth roles of interleukin (IL)-6 and toll-like receptor (TLR)4 signaling in late-OA SF using healthy $CD14^+$ monocytes. Classical IL-6 signaling immunosuppressed $CD14^+$ monocytes via signal transducer and activator of transcription (STAT3) and suppressor of cytokine signaling (SOCS3), while TLR4 via nuclear factor kappa-light-chain-enhancer of activated B (NF-κB) and c-Jun Terminal Kinase (JNK) drove $CD14^+$ monocyte activation in late-OA SF. Addition of marrow-derived MSC(M) soluble factors enhanced immunosuppression through IL-6 signaling and nullified late-OA SF activation effects by decreasing p-JNK and reducing TLR-mediated NF-κB and TNF. MSC(M) immunosuppressed $CD14^+$ monocytes in late-OA SF were also functionally rescued with improved phagocytosis. We thus demonstrated that soluble factors from MSC(M) mitigate the activating effects of late-OA SF through IL-6 dependent and independent

pathways resulting in CD14^{+} monocytes with increased immunosuppressive phenotypes and function.

Graphical Abstract

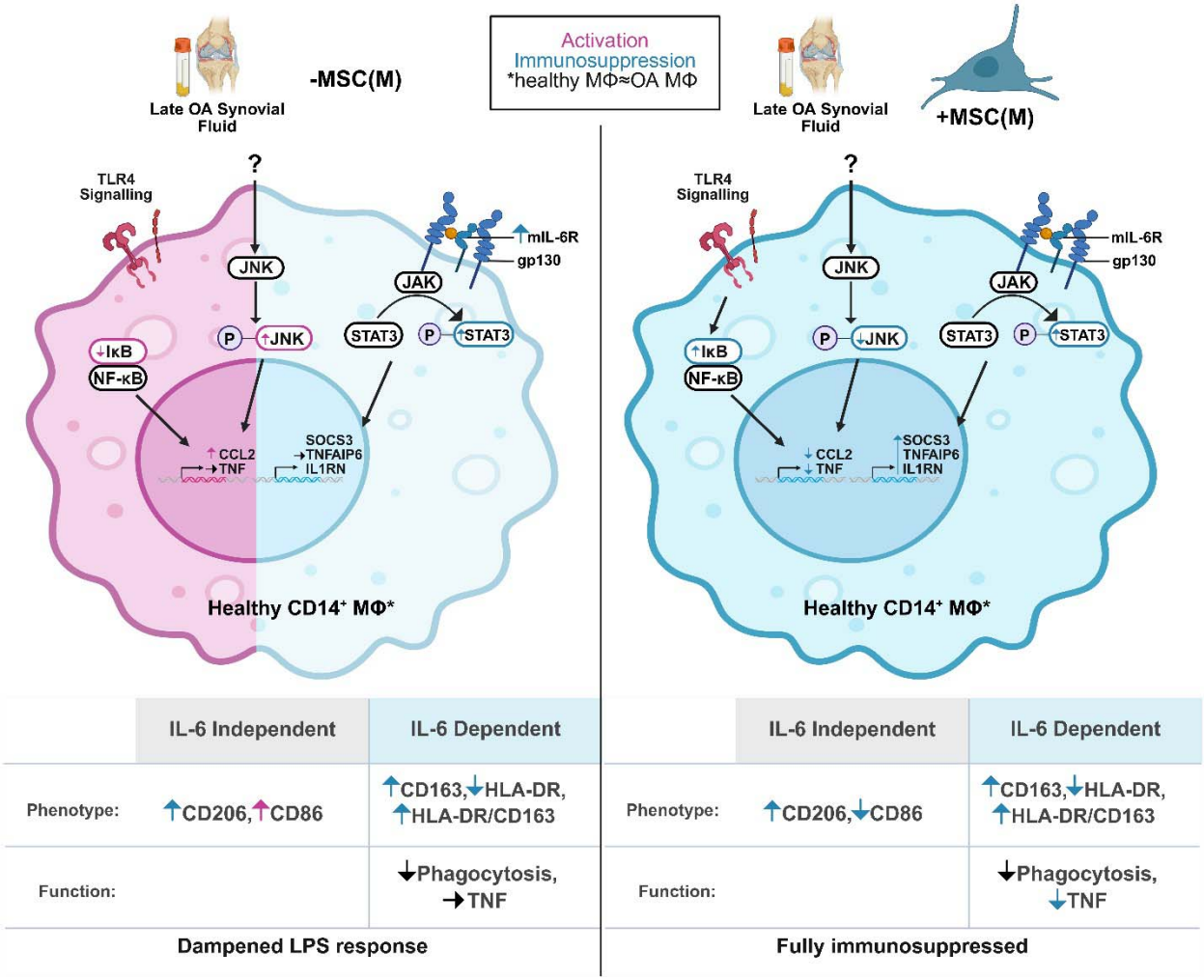

	IL-6 Independent	IL-6 Dependent
Phenotype:	↑CD206,↑CD86	↑CD163,↓HLA-DR, ↑HLA-DR/CD163
Function:		↓Phagocytosis, →TNF
Dampened LPS response		

	IL-6 Independent	IL-6 Dependent
Phenotype:	↑CD206,↓CD86	↑CD163,↓HLA-DR, ↑HLA-DR/CD163
Function:		↓Phagocytosis, ↓TNF
Fully immunosuppressed		

Introduction

Osteoarthritis (OA) is a chronic, low-grade inflammatory condition that affects over 15% of the global population (1). Iinflammation of the synovium lining, or synovitis (2) contributes significantly to OA pathology (3,4) and is mediated by monocytes/macrophages (MΦs), which are the most prevalent immune cells in knee OA (KOA) patients (5,6). An enrichment of $CD14^{+}CD16^{+}$ intermediate synovial fluid (SF) MΦ subsets correlates with worsening patient-reported outcome measures (PROMs) including knee osteoarthritis outcome scores (KOOS) in KOA patients. Mechanisms for the increase in the intermediate subset and its functional roles in KOA have not been fully investigated.

In parallel, treatment of KOA with mesenchymal stromal cells (MSC) has shown mixed clinical efficacy (7) with undetermined mechanisms of action; MSC reduce inflammation (7,8) and interact with MΦs (9,10). KOA SF is complex, containing multiple factors that license MSC, triggering their immunomodulatory activities. MSC(M) licensed by KOA SF produce elevated levels of IL-6 (11), a pleiotropic cytokine with cell- and disease-specific roles (12), including pro-resolving effects on MΦs (13). Paradoxically, IL-6 is associated with radiographic KOA (14), increased pain, and worsening function in KOA patients (15). Given that MSC result in analgesic and function-preserving effects (7), MSC-secreted IL-6 is hypothesized to play a regulatory role in the context of KOA.

We show that SF MΦs are tolerized based on in vitro LPS re-challenge. Longer-term exposure of surrogate $CD14^+$ peripheral monocytes from healthy or OA patient donors to late-OA SF induces only partial tolerization. Additionally, late-OA SF matrix activates, immunosuppresses, and functionally impairs $CD14^+$ peripheral monocytes. Using phenotypic markers, signaling kinases, and functional readouts, we elucidate roles of canonical IL-6 signaling in late-OA SF immunosuppression of $CD14^+$ peripheral monocytes; and roles for the TLR4-mediated NF-κB pathway and JNK pathway that contribute to $CD14^+$ monocyte activation. While LPS re-challenge does not fully replicate endotoxin-induced in vitro tolerization, there is partial tolerance. Addition of MSC(M) enhances the IL-6 mediated immunosuppressive effects and negates the late-OA SF activation effects. Importantly, MSC(M) educated $CD14^+$ monocytes from healthy donors have reduced TNF and improved phagocytosis and functionality.

Results

Late-Stage OA SF contains MΦs with a mixed phenotypic profile

SF from mid-stage and late-stage (Table S1) KOA patients showed increases in cytokines, chemokines and alarmins (Table 2) based on the area under the ROC curve of ≥ 0.74 (Fig. S1A-D). IL-6 and CCL2 increased in late-OA SF vs. non-OA SF but not mid-OA SF (Fig. 1A,B), while S100A8/9 and IL-8 significantly increased from mid-to late-stage OA SF (Fig. 1C,D). MΦs from late-OA SF were immunophenotyped; classical $CD14^+CD16^{neg}$ and intermediate $CD14^+CD16^+$ MΦs subsets were the most abundant, as before (6) (Fig. 1E). Classical, intermediate and non-classical SF MΦs all expressed

CD163, CD206 and Human Leukocyte Antigen-DR isotype (HLA-DR), albeit at varying ratios (Fig. 1F-H). SF MΦs showed increased expression of CD163, CD206 and HLA-DR, although the balance was tipped towards a reduced HLA-DR/CD163 mean fluorescence intensity (MFI) expression ratio (Fig. 1I), suggestive of tolerized, intermediate SF MΦs. There were no significant differences in CD163 and HLA-DR expressions between classical and non-classical MΦ subsets, although the classical but not non-classical MΦ subset had increased HLA-DR/CD163 ratios (Fig. 1F,H,I).

Short-term challenge with lipopolysaccharide (LPS) with or without additional tolerization showed no significant phenotypic or intracellular IL-1 and TNF expression changes, suggestive of in vivo tolerization of SF MΦs by late-OA SF; MΦs were not further tolerized or challenged in vitro (Fig. 1J).

***CD14$^+$ peripheral monocytes exposed to OA SF, as a surrogate for OA SF* MΦs**

To perform more detailed analyses on intermediate SF MΦs, we require 5×10^6 MΦs/run. We routinely isolate 3-10 $\times 10^4$ SF MΦs, insufficient for multivariate analyses without further cell culturing and culture induced modifications. To circumvent this limited supply, peripheral CD14$^+$ monocytes from healthy donors were isolated and exposed to mid- or late-OA SF for 3 days. This increased the frequency of intermediate and decreased classical monocyte subsets (Fig. 2A; S2A), mimicking the frequency changes of SF MΦs (6).

Peripheral $CD14^+$ monocytes from healthy vs. OA patients had comparable basal phenotypic changes to longer-term exposure to late-OA SF and exhibited partial, albeit different tolerization effects with additional LPS re-challenge (Fig. 2B). Healthy and OA $CD14^+$ monocytes in late-OA SF had unchanged CD163, CD86 after LPS-rechallenge (Fig. 2B). CD206 and HLA-DR were increased in healthy $CD14^+$ monocytes, but unchanged in OA $CD14^+$ monocytes while TNF was non-significantly and significantly increased in healthy vs. OA $CD14^+$ monocytes, respectively (Fig. 2B). Importantly, healthy and OA $CD14^+$ monocytes in late-OA showed unchanged HLA-DR/CD163 ratios with LPS rechallenge, arguing for overall similar partial tolerization profiles (Fig. 2C). We highlight data in response to late-OA SF in both OA and healthy $CD14^+$ monocytes but focused on healthy $CD14^+$ monocytes for in-depth analysis, given their ready availability and comparable profiles to OA $CD14^+$ monocytes (Fig. 2B).

Increase in the percentage of healthy $CD14^+CD16^+$ monocytes by exposure to mid- or late-OA SF was abrogated by an IL-6 neutralizing antibody (16) (Fig. 2D; S2B), suggestive of endogenous IL-6 stimulation within OA SF. $CD14^+$ monocytes treated with supraphysiological levels of IL-6 as a positive control showed increased CD163 and CD206 (Fig. 2E,F) and decreased HLA-DR/CD163 ratios (Fig. 2I) without effects on HLA-DR or CD86 (Fig. 2G,H). Late-OA SF addition to healthy and OA $CD14^+$ monocytes mimicked supraphysiological IL-6 effects on CD163, CD206, HLA-DR (Fig. 2B,E-G) and the HLA-DR/CD163 ratio (Fig. 2C,I). Late-OA SF, unlike supraphysiological IL-6 significantly increased CD86 expression in healthy but not OA $CD14^+$ monocytes, relative to untreated controls (Fig. 2B,H).

The effects of IL-6 and other factors in late-OA SF were further studied in healthy $CD14^+$ monocytes. Neutralizing IL-6 antibody nullified late-OA SF effects on CD163 and HLA-DR/CD163 ratio (Fig. 2E,I) but not CD206, HLA-DR, or CD86 on $CD14^+$ monocytes (Fig. 2F-H), suggestive of IL-6-dependent and independent effects. Mid-OA SF had similar albeit insignificant trends (Fig. 2E-I). S100A8/9, an endogenous TLR ligand, in late-OA SF reduced CD163, CD206 and CD86, compared to late-OA SF stimulation, with a concomitant increase in HLADR/CD163 ratio (Fig. S2D-H). Therefore, physiological levels of S100A8/9 did not replicate the phenotypic effects of late-OA SF on healthy $CD14^+$ monocytes. Addition of a TLR inhibitor, TAK242 (17) to late-OA SF also did not abrogate phenotypic effects of endogenous S100A8/9 in late-OA SF (Fig. S2D-H).

Functionally, late-OA SF with LPS re-challenge showed non-significantly increased TNF production compared to late-OA SF alone, confirming only partial tolerization effects of healthy $CD14^+$ monocytes (Fig. 2J). Supraphysiological IL-6 significantly reduced, while IL-6 antibody with late-OA SF significantly increased TNF production, confirming an endogenous IL-6 effect in late-OA SF (Fig. 2J). S100A8/9, while not mimicking late-OA SF phenotypic effects, replicated late-OA SF effects on TNF production; TAK242 significantly suppressed TNF production (Fig. S2I). We thus identify a role for TLR4 pathway in TNF production in late-OA SF. TNF production by mid (vs. late) OA SF stimulation was significantly lower (Fig. 2J), confirming reduced pro-inflammatory mediators in mid- vs. late-OA SF (Fig. 1A-D).

IL-6 signaling in OA SF is mediated through canonical, not trans-signaling

IL-6 canonical signaling occurs through membrane IL-6 receptor (mIL-6R) while trans-signaling occurs through soluble IL-6 receptor (sIL-6R) and gp130 (Fig. 3A). IL-6 increased from mid- to late-stage OA (Fig. 1A) but sIL-6R levels decreased (Fig. 3B), arguing against IL-6 trans-signaling. To clarify whether IL-6 signaling to healthy $CD14^+$ monocytes in late-OA SF was through canonical- or trans-signaling, we added physiological levels of IL-6 with or without physiological sIL-6R; there were no significant phenotypic changes in healthy $CD14^+$ monocytes, supportive of the absence of competitive trans-signaling (Fig. 3C-F). This was replicated by addition of soluble gp130 (sgp130) in the presence of late-OA SF (Fig. 3C-F). Additionally, mIL-6R expression increased on $CD14^+$ monocytes exposed to mid- or late-OA SF (Fig. 3G), confirming dominance of classical IL-6 signaling. There was a complete absence of detectable IL-6-sIL-6R complexes in both mid- and late-OA SF (undetectable in 91 of 96 samples), readily found in inflammatory arthritic controls (Fig. 3H).

Temporally sensitive activation of signaling pathways in $CD14^+$ monocytes

We noted extensive activation of mitogen-activated protein kinase (MAPK) and STAT kinases in healthy $CD14^+$ monocytes treated with late-OA SF using a phospho-kinase array (Fig. S3A). Although multiple MAP kinases were evaluated, only significant changes in the phosphorylation (p) levels of c-Jun Terminal Kinase (JNK) were observed (Fig. S3B-D). Temporal regulation of p-JNK and p-STAT3 were identified (Fig. S3D,E).

Kinase activation by IL-6 or S100A8/9 in healthy $CD14^+$ monocytes was investigated by pre-treatment with neutralizing IL-6 antibody or TLR inhibitor, TAK242 followed by late-OA SF for short- or longer-exposures (Fig. 4A). Controls included treatment with IL-6 or S100A8/9 for short (40 min, Fig. S3F) and longer exposures (24h; Fig. 4A). Short-(Fig. 4B,D) and longer- (Fig. 4C,D) exposures to IL-6 significantly but differentially increased normalized p-STAT3 levels. Short- and longer-exposures to late-OA SF also increased normalized p-STAT3 (Fig. 4B-D), although only longer-exposure times mimicked supraphysiological IL-6 (Fig. 4C,D). Conversely, S100A8/9 reduced normalized p-STAT3 at longer- and short-exposures, relative to late-OA SF (Fig. 4B-D; S3F), confirming that S100A8/9 does not fully re-capitulate late-OA SF effects. Pre-treatment with IL-6 antibody also reduced normalized p-STAT3 at both longer- and short-exposures (Fig. 4B,D). TAK242, on the other hand, significantly elevated normalized p-STAT3 levels at short- but not longer-exposures (Fig. 4B-D). TAK242 inhibition thus replicates differential IL-6 short- vs. longer-term effects and overrides S100A8/9-mediated inhibition of STAT3 phosphorylation (Fig. 4B-D; S3F). Together, these data support IL-6- and TAK242-mediated increases p-STAT3 in the short- but not longer-exposures, suggestive of feedback mechanisms.

By contrast, IL-6 or S100A8/9 stimulation did not significantly alter normalized p-JNK at short- or longer-exposures, implicating other factors in late-OA SF for observed p-JNK activation (Fig. 4B,C,E). Pre-treatment with IL-6 antibody significantly decreased normalized p-JNK at short-exposures. Longer-exposures to late-OA SF reversed IL-6 antibody effects, restoring p-JNK to short-exposure levels of late-OA SF. This suggests

longer-term late-OA SF tolerization effects on p-JNK that are not susceptible to IL-6 modulation. Conversely, TAK242 inhibition in late-OA SF increased normalized p-JNK levels at short- but not longer- exposures; longer TAK242 exposures mimicked late-OA SF tolerization (Fig. 4B,C,E). JNK inhibition by SP600125 reduced p-JNK and p-STAT3, which was overridden by addition of late-OA SF, suggesting complex, temporally regulated inhibitory interplay between STAT3 and JNK phosphorylation (Fig. S3G).

Canonically, nuclear factor of kappa light polypeptide gene enhancer in B-cells inhibitor alpha (IκBα) inhibits bound NF-κB; it is degraded in the cytosol and releases NF-κB (18). IL-6 increased normalized levels of IκBα at short- and longer- exposures relative to late-OA SF stimulations; the effects of endogenous IL-6 in late-OA SF were reversed by IL-6 antibody (Fig. 4B,C,F). S100A8/9, however, mimicked late-OA SF, especially at short- vs. longer exposures, reducing normalized IκBα levels; TAK242 in late-OA SF rescued IκBα (Fig. 4B,C,F).

Differential kinetics of IL-6-mediated short- vs. longer-exposures indicated feedback inhibition including suppressor of cytokine signaling 3 (SOCS3), a known modulator of IL-6 signaling (19). As expected, SOCS3 increased after longer IL-6 exposure (Fig. 4G). Surprisingly, SOCS3 and p-STAT3 both increased with longer late-OA SF exposure (Fig. 4D,G). IL-6 antibody with late-OA SF dually reduced SOCS3 and p-STAT3 (Fig. 4D,G). Longer-term exposure to S100A8/9 similarly reduced SOCS3 and p-STAT3 (Fig. 4D,G); shorter S100A8/9 exposures also attenuated p-STAT3 even in the presence of

supraphysiological IL-6 and late-OA SF (Fig. S3F). TAK242 reversed the effects of endogenous S100A8/9 in late-OA SF, given known S100A8/9 binding to TLR4 ((20); Fig. 4B,D, G; S3F). Thus, differential STAT3 phosphorylation by various treatments in late-OA SF is not fully explained by SOCS3 upregulation and indicates other contributing effectors.

CCL2, downstream of JNK and IL-6 (21), may be one such effector. CCL2 was increased by longer exposures to late-OA SF and TAK242 and decreased by IL-6 antibody (Fig. 4H). Changes to CCL2 correlated with JNK phosphorylation mediated by short late-OA SF exposures, with or without IL-6 antibody or TAK242 inhibition (Fig. 4E, H). However, there were no correlations between CCL2 and JNK phosphorylation with longer exposures to late-OA SF (Fig. 4E, H), indicative of other mediators.

TNF, downstream of JNK and NF-κB (22,23) was slightly, but not significantly increased by late-OA SF, concordant with partial tolerization effects of late-OA SF; however, it was inversely correlated with the opposing effects of IL-6 and S100A8/9 on IκBα (Fig. 4F,I). IL-6 antibody increased TNF, correlating with reduced IκBα activation; TAK242 decreased TNF, correlating with increased IκBα (Fig. 4F,I).

Longer late-OA SF exposures activated STAT3 and JNK phosphorylation without changes to SOCS3; reduced IκBα with elevated CCL2; and non-significantly increased

TNF. Together with other downstream effectors, this resulted in a mixed activated, immunosuppressed, semi-tolerized, $CD14^+$ monocyte profile in late-OA SF.

MSC(M) countered late-OA SF effects on $CD14^+$ monocytes

Healthy and OA $CD14^+$ monocytes co-cultured directly with MSC(M) alone show increased CD163, reduced HLA-DR, CD86 and HLA-DR/CD163 MFI ratio (Fig. 5A-C). MSC(M) with late-OA SF synergistically and significantly increased CD163 and CD206 (Fig. 5A-C) and reduced HLA-DR and HLADR/CD163 MFI ratios (Fig. 5A-C) in healthy and OA $CD14^+$ monocytes, confirming additional immunosuppressive effects.

Next, we tested tolerization effects of MSC(M) by re-challenging healthy vs. OA $CD14^+$ monocytes with LPS, with and without late-OA SF. MSC(M) further reduced HLA-DR and CD86 MFI in LPS-stimulated conditions, with and without late-OA SF exposure (Fig. S4F, G). However, healthy vs. OA $CD14^+$ monocytes were comparable in late-OA SF with LPS re-challenge, both in the presence and absence of MSC(M). This confirms partial tolerization of healthy and OA $CD14^+$ monocytes by late-OA SF exposure and similar immunosuppression, but not tolerization by MSC(M).

Given similar responses of OA vs. healthy $CD14^+$ monocytes to MSC(M) in late-OA SF, we conducted an in-depth analysis on healthy $CD14^+$ monocytes. IL-6 antibody reversed MSC(M) mediated effects on CD163, HLA-DR MFI, but not on CD206 or CD86 or HLA-DR/CD163 MFI ratio (Fig. 5D-H). S100A8/9 addition did not reverse MSC(M) phenotypic effects (Fig. S4A-E).

18-21% of MSC(M) in late-OA SF demonstrated early apoptosis, a significant increase over controls; this was a donor-dependent effect (Fig. S5A). IL-6 antibody rescued the late-OA SF apoptosis; S100A8/9 did not potentiate MSC apoptosis arguing for other responsible factors in late-OA SF.

Next, we tested MSC(M) soluble factors. Secondary healthy or OA $CD14^+$ monocytes were treated with conditioned medium (CM) from primary direct co-cultures of corresponding healthy vs. OA $CD14^+$ monocytes with MSC(M), licensed by late-OA SF (Fig. 6A). Normalized p-STAT3 and IκBα levels significantly increased by licensed MSC(M) CM; normalized p-JNK was reduced significantly, relative to late-OA SF alone, despite the long-term exposure (Fig. 6B-D). Licensed MSC(M) CM significantly attenuated TNF, even with LPS re-challenge in both OA and healthy $CD14^+$ secondary monocytes (Fig. 6D).

Given similar responses to MSC(M) CM, in-depth analyses were conducted on healthy $CD14^+$ monocytes. Pre-treatment with an IL-6 antibody reduced p-STAT3, increased p-JNK, without effects on normalized IκBα (Fig. 6B, E-G). Licensed MSC(M) CM increased p-STAT3 and reduced p-JNK in an IL-6-dependent manner while increasing IκBα in an IL-6-independent manner.

Downstream effectors, including SOCS3, were significantly upregulated by late-OA SF licensed MSC(M) CM (Fig. 6H), mimicking supraphysiological IL-6 (Fig. 4G). IL-6 antibody nullified this increase, confirming IL-6-mediated MSC(M) soluble effects (Fig.

6H). Licensed MSC(M) CM also increased IL-6 downstream genes, including TNF-alpha Induced Protein 6 (TNFAIP6), IL-1 Receptor Antagonist (IL1RN) and prostaglandin-endoperoxide synthase 2 (PTGS2) (Fig. S5B,C,D). CCL2 and TNF were suppressed by late-OA-SF licensed MSC(M), with TNF gene and protein, but not CCL2, demonstrating IL-6-dependency (Fig. 6I-K).

$CD14^+$ monocytes in late-OA SF licensed MSC(M) CM were larger, more spindle-shaped and took on a macrophage appearance (Fig. S5E). Late-OA licensed MSC(M) CM also rescued phagocytotic activity, which was reduced by late-OA SF exposure, in an IL-6 dependent manner (Fig. 6L).

Discussion

We evaluated immunosuppression and activation of OA and healthy $CD14^+$ peripheral monocytes exposed to complex mixture of activating, suppressing and tolerizing factors in late-OA SF, in the presence or absence of MSC(M) to understand the basal profile of monocytes in OA SF, and the rescue effects of MSC(M). Insights from this study thus provides mechanistic basis for clinically reported MSC(M) analgesic and functional improvement effects in KOA patients (7,10).

We used peripheral $CD14^+$ monocytes exposed to late-OA SF to study MSC(M) interactions with SF MΦs, given their limited availability. MSC(M) reduce $CD14^+CD16^+$ intermediate SF MΦ frequency in KOA patients (10), which correlate inversely with KOA

PROMs (6). CD14$^+$ peripheral monocytes in late-OA SF had IL-6 dependent increases in frequency of intermediate monocytes, concordant with activated monocytes exposed to inflammatory disease stimuli (24–26). However, healthy and OA patient peripheral CD14$^+$ monocytes exposed to late-OA SF were also semi-tolerized, like peripheral monocytes in active sepsis (27). Healthy and OA CD14$^+$ monocytes showed similar HLA-DR/CD163 profile; similar phenotypic and signaling kinase activation responses to MSC(M), boosting confidence in the extendibility of results from healthy to OA CD14$^+$ monocytes. However, there were subtle differences indicative of altered tolerization profiles likely from systemic effects of KOA; healthy CD14$^+$ monocytes in late-OA SF and LPS re-challenge had increased HLA-DR, unchanged CD86 expression and non-significant increases in TNF production, while OA CD14$^+$ monocytes had unchanged HLA-DR, CD86 expression and significant increase in TNF production. Both OA and healthy CD14$^+$ monocytes were thus only partially tolerized; neither demonstrated classic endotoxin tolerization nor mimicked endogenous SF MΦs, which were fully tolerized, as others reported (28).

Late-OA SF contains numerous factors including IL-6, alarmins, endotoxins (29–31); variable levels of pro-inflammatory cytokines (5,32); complement activators (33), ECM fragments (34). These multiple factors exist in dynamic, fluctuating ratios and thus induce a mixed activated, immunosuppressed and partially tolerized CD14$^+$ peripheral monocyte profile.

MSC(M), licensed by factors present in OA SF, secrete high levels of IL-6 (11), IL-6 has paradoxical roles; IL-6 correlates with increased OA severity and incidence (15,35,36). IL-6 knockout mice develop more severe spontaneous OA (37), while IL-6 knockout experimental OA models show increased cartilage damage (38), supportive of context-dependent IL-6 signaling in OA.

IL-6 binds to IL-6R, dimerizes gp130 and induces classical signaling (39). Classical signaling, tightly regulated by SOCS3 (40) is restricted to hepatocytes and leukocytes which express IL-6R (41–43), and results in anti-inflammatory effects (44). Signaling through sIL-6R, generated by proteolytic cleavage of mIL-6R or through transcription of alternatively spliced IL-6R mRNA (45,46) results in trans-signaling (47), which is broader given the ubiquitous expression of gp130 receptors; trans-signaling results in stronger activation of intracellular signaling (48) and is reported to be pro-inflammatory (44).

We are the first to report SF levels of sIL-6R in KOA patients vs. non-OA samples. sIL-6R levels decreased with OA progression; there was an absence of detectable sIL-6R-IL-6 complexes in OA SF. Our data thus supports IL-6 classical signaling to $CD14^+$ monocytes, which express mIL-6R (51) in late-OA SF via p-STAT3 and SOCS3. IL-6 antibody with longer late-OA SF exposure reduced SOCS3 and p-STAT3 but increased p-JNK. We show co-variance of SOCS3 and p-STAT3, contrary to reported inverse

correlations (50). This may be because we measured SOCS3 at the transcript level, and/or this may indicate partial tolerization effects of late-OA SF.

We also explored alarmins and showed they could only partially recapitulate late-OA SF effects. S100A8/9 did not replicate JNK activation by late-OA SF. TAK242 increased short- but not longer-term JNK phosphorylation in late-OA SF. S100A8/9, however replicated late-OA SF, decreasing IκBα; this was reversed by TAK242, but accompanied by increases in CCL2. This may be explained by alternate pathways including phosphatidylinositol 3-kinase (PI-3K)/Akt (52). Thus, we postulate canonical TLR4 signaling (53) in late-OA SF through NF-κB but not JNK pathways.

We also observed an interplay between TLR-mediated short-term effects on JNK and STAT3 and long-term effects of IL-6 signaling on STAT3 and JNK, consistent with previous reports (54).

Healthy and OA $CD14^+$ monocytes exposed directly to MSC(M) in late-OA SF had enhanced immunosuppression and reduced activation. Mid-vs. late-OA SF licensed MSC(M) produced similar phenotypic profiles, but without significant reductions in HLA-DR indicative of altered ratios of mediators in mid- vs. late-OA SF.

Given that 18-21% of MSC(M) were undergoing early apoptosis with exposure to late-OA SF, we cannot rule out efferocytosis of MSC(M) by $CD14^+$ monocytes under direct culture as previously reported (9,55,56). However, late-OA SF licensed MSC(M) CM showed differences in signaling kinases, genes, phagocytosis and TNF production by secondary $CD14^+$ monocytes, speaking to the effects of MSC(M) soluble factors.

IL-6 classical signaling from late-OA SF licensed MSC(M) CM dually increased p-STAT3 and SOCS3*,* thereby attenuating the mixed effects of late-OA SF, and partially explaining MSC(M) beneficial effects. Longer exposures to late-OA SF did not change SOCS3*,* but increased p-STAT3, mirroring SOCS3-dependent MSC mitigation of LPS-activation of alveolar macrophages (57).

Soluble factors in late-OA SF licensed MSC(M) CM also acted through the JNK/STAT3 axis by reducing p-JNK, increasing p-STAT3 and IκBα levels. These soluble factors increased TNFAIP6 *e*ncoding for TNF-stimulated gene 6 protein (TSG-6), PTSG2*,* which encodes cyclooxygenase (58) and IL1RN in secondary $CD14^+$ monocytes. TSG-6, an important MSC immunoregulator (59), inhibits JNK and NF-κB activation and promotes transition to anti-inflammatory macrophages (60,61). Cyclooxygenase converts arachidonic acid to prostaglandin (PG). Although PG is associated with OA pathology (62,63), dual roles for PG have been reported including attenuation of inflammatory genes (64). Increased IL-1R antagonist has demonstrated protective effects in animal models of OA.

$CD14^+$ monocytes took on a differentiated macrophage morphology in the presence of late-OA SF, and even more so with late-OA licensed MSC(M) CM. However, $CD14^+$ monocytes are semi-tolerized with late-OA SF exposure with impaired functionality as measured by phagocytosis, congruent with disrupted efferocytosis of peripheral macrophages in OA patients (65). Licensed MSC(M) CM rescued phagocytotic capacity.

This study has a few limitations. We could not directly assess SF MΦs, due to limited KOA SF cellular content. Healthy and OA peripheral $CD14^+$ monocytes, treated with OA SF were used to mimic SF MΦs. Although SF MΦs were more tolerized, studying $CD14^+$ peripheral monocytes in late-OA SF was useful to understand cellular mechanisms without confounding effects of other joint cell types.

We conducted detailed analyses with IL-6, S100A8/9 and TAK242 on healthy $CD14^+$ monocytes, which exhibited similar basal profiles as OA $CD14^+$ monocytes in response to late-OA SF, but slight differences in terms of tolerization profile with LPS re-challenge. The availability of healthy vs. OA patient $CD14^+$ monocytes drove this decision. However, comparable basal phenotypic and kinase activation profiles of healthy and OA $CD14^+$ monocytes to late-OA SF stimulation substantiates the generalizability of our findings. Importantly, responses of healthy and OA $CD14^+$

monocytes to MSC(M) were similar, validating transferability of mechanisms gleaned from healthy to OA $CD14^+$ monocytes.

Although MSC(M) mimicked IL-6 classical signaling, and mitigated some S100A8/9 effects, neither fully reproduced the extent of MSC(M) immunosuppressive effects. This is highly suggestive of other MSC soluble factors, including PTSG2, TNFAIP6, and IL1RN, which are elevated in $CD14^+$ monocytes by late-OA SF-licensed MSC (M) CM and may ultimately be responsible for the observed immune suppression.

MSC(M) through IL-6 classical signaling, further immunosuppressed, already semi-tolerized peripheral $CD14^+$ monocytes in late-OA SF. MSC(M) also modulated $CD14^+$ monocytes in late-OA SF in an IL-6 independent manner, likely through TLR4 signaling. MSC(M) promoted $CD14^+$ macrophage differentiation and rescued phagocytotic functionality. Our data thus provides mechanisms of licensed MSC soluble factors that generate an immune-suppressed, $CD14^+$ monocyte profile in late-OA SF, reminiscent of absolutely tolerized macrophages (66).

Materials and methods

SF sample collection

SF samples were either collected from patients diagnosed with KOA (n=139, REB 14-7483) or from non-OA screened cadaveric donors (n=11, REB 24-566). Cadaveric

samples were provided by collaborator, R Krawetz. Patients with KOA had up to 5 mL of SF aspirated at the time of clinical intervention (prior to intra-articular injection, arthroscopy, or arthroplasty). KOA patients met the American College of Rheumatology criteria for symptomatic KOA (67). Radiographs from patients were used for KL grading. Demographic information on patients and their KL grading is in Table S1. Psoriatic arthritis (n=2) and rheumatoid arthritis SF sample (n=1) were collected under REB 21-5591 and REB14-7483, respectively.

SF MΦs immunophenotyping

Collected SF samples were stored at 4□°C and processed within 24 hours of acquisition. Samples exhibiting visible blood contamination were excluded. SF MΦs were isolated and immunolabeled using a previously established protocol (6). For the tolerization study, isolated SF MΦs were cultured in the presence or absence of lipopolysaccharide (LPS, 10 ng/mL) for 48h and restimulated with 10 ng/ml LPS for 4h. Details of the antibodies used for MΦ immunophenotyping and intracellular staining are provided in Table S3.

Isolation of CD14$^+$ monocytes and MSC(M)

Human peripheral blood mononuclear cells (PBMCs) were isolated from the whole blood of healthy donors or late-stage OA patients (REB14-7483) using density gradient centrifugation. CD14$^+$ monocytes were purified via magnetic sorting using CD14$^+$ MicroBeads (Miltenyi Biotec), following the manufacturer's protocol (68). CD14$^+$ monocytes were cryopreserved until use. CD14$^+$ monocytes were cultured in RPMI1640

medium supplemented with 10% fetal bovine serum, 1% sodium pyruvate, and 1% penicillin-streptomycin (Gibco). Each experimental condition included three independent biological donors with three technical replicates.

MSC(M) were isolated from bone marrow aspirates obtained from the iliac crest of healthy donors (REB 16-5493) and expanded as before (69). MSC(M) were thawed three days before experiments at passage 4. MSC(M) were characterized as before (11). Three biological donors were used (Table S1).

Evaluation of soluble factors in SF and cell culture medium by Enzyme-linked immunosorbent assay (ELISA)

Clear SF samples after centrifugation (12,000xg for 15 min) or conditioned medium (CM) were stored at -80ºC until analysis. IL-6, CCL2, S100A8/9, IL-6-sIL-6R, sIL-6R, IL-8 and TNF were detected using the ELISA kit manufacturer's instructions and diluted with kit-specific solutions (as detailed in Table S4). For TNF assays, cells were re-stimulated with LPS (*E. coli* origin, 2.5 ng/mL; Millipore-Sigma) for 4 hours before collecting the CM at 48h.

$CD14^+$ monocyte and MSC(M) culture and treatments

$CD14^+$ monocytes (2.5 × 10□ cells) were cultured in 24-well plates in a total volume of 400 µL. $CD14^+$ monocytes were treated with human recombinant IL-6 at concentrations of 0.5, 5, 10, and 50 ng/mL (PeproTech, 200-06); S100A8/9 at 1 µg/mL (R&D Systems, B226-S8); sIL-6R (Cedar Lane, CLCYT286) at 10 ng/mL, and sgp130 (R&D Systems,

228-GP) at 10 ng/mL. Pooled mid- or late-stage OA SF, collected from eight patients, was used at 30% (v/v%) for each set of experiments. For inhibitors, $CD14^+$ monocytes were pre-treated for 1 hour with IL-6 neutralizing antibody (2.5 µg/mL; R&D Systems, MAB206), or TAK-242 (1 µM/mL; Millipore-Sigma, 5.08336), or SP600125 (50 nM/mL; Adooq Bioscience, A21502). Short-term exposure times were variable and consisted of $CD14^+$ monocytes treatment with recombinant IL-6 (5 ng/mL) or S100A8/9 (1 µg/mL) for 40 minutes, or with 30% (v/v) pooled late-stage OA SF for 1 hour. Long-term exposures consisted of the same stimuli for 24 hours (Fig. 4A).

$CD14^+$ monocytes were co-cultured directly with MSC(M) at a 5:1 ratio with indicated conditions for 72 hours. $CD14^+$ monocytes in co-cultures with MSC(M) were licensed with mid- or late-stage OA SF, with or without pre-treatment (for 1h) with IL-6 neutralizing antibody (Fig. 5A). Healthy or late-stage OA $CD14^+$ monocyte tolerization was assessed only via direct co-cultures with and without MSC(M) in late-stage OA SF for 72h, followed by an additional 4-hour LPS re-challenge. Conditioned medium, termed as late-OA SF licensed MSC(M) CM, containing soluble factors from these co-cultures, was centrifuged at 1,000g for 5 min and stored at −80 °C for subsequent use in secondary $CD14^+$ monocyte cultures for downstream analysis, including western blotting, gene and soluble TNF assessments (Fig. 6A).

MSC(M) were treated with late-OA SF for 1h, 24h, 48h and 72h, and the percentage of early apoptotic cells was subsequently assessed by flow cytometry. Cells were harvested using TrypLE (Gibco), followed by staining with the Annexin V-FITC

Apoptosis Detection Kit with 7-AAD (Biolegend, Cat# 640922), according to the manufacturer's instructions. Early apoptosis was determined as the percentage of Annexin V^+ within the live, 7-AAD-negative MSC(M).

$CD14^+$ monocytes flow cytometry

For flow cytometric analysis, $CD14^+$ monocytes were harvested after 72 hours of treatment, washed with sterile phosphate-buffered saline (PBS) and immunolabeled with antibodies against CD45, CD14, CD16, and either CD163, CD206, HLA-DR, CD86, or mIL-6R, as listed in Table S3. $CD45^+$ monocytes were classified based on the expression of CD14 and CD16 (Fig. S2A). The MFI was quantified using FlowJo analysis software version 10.10. The MFI of each cell surface marker on treated $CD14^+$ monocytes was normalized to the donor-matched average MFI value of the corresponding marker measured in three technical replicates of untreated $CD14^+$ monocytes. Normalized MFI values from three biological replicates were analyzed across different treatment conditions.

Western blot analysis

$CD14^+$ monocytes cultured for short and longer-term exposures (Fig. 4A and 6A) were lysed using previous protocols (70). 15 µg of cell lysates were subjected to electrophoresis on a 10% polyacrylamide gel and transferred to polyvinylidene fluoride (PVDF) membranes. Membranes were blocked and immunoblotted with indicated primary antibodies (Table S5), diluted 1000-fold. The blots were washed with Tris-based saline-tween 20 (TBS-T) and incubated with secondary horseradish peroxidase (HRP)-

conjugated antibodies (Cell Signaling) in 5% skim milk. After washing the membranes in TBS-T, the signal was detected with the enhanced chemiluminescence reagent (ThermoFisher Scientific) and a Bio-Rad chemiluminescent imaging system. The images were quantified with ImageJ analysis software. Phosphorylated kinases were normalized for glyceraldehyde-3-phosphate dehydrogenase (GAPDH) or corresponding total protein.

Gene expression analysis

After 48h of exposure under indicated conditions, $CD14^+$ monocytes were collected for gene expression readouts. Total RNA from treated $CD14^+$ monocytes was extracted with TrIzol reagent (Life Technologies). cDNA was synthesized using SuperScript IV VILO master mix (ThermoFisher Scientific) per the manufacturer's instructions. The primer sequences are listed (Table S6). A PCR detection system (Q5; ThermoFisher Scientific) with the following cycling parameters: initial denaturation at 95 °C for 60 s, followed by 40 cycles of 95°C for 10 s and 60°C for 30s was used. The levels of target mRNA were normalized to three housekeeping mRNA levels of GAPDH, beta-2-microglobulin (B2M) and β-Actin using the $2^{-\Delta\Delta Ct}$ method.

Phagocytosis

$CD14^+$ monocytes were differentiated into macrophages over 5 days in the presence of 20 ng/mL M-CSF (PeproTech). Macrophages (1 × 10□ cells per well) were seeded in 96-well plates and treated for an additional 3 days with M-CSF (20 ng/mL), with or without either late-stage OA SF, or CM from late-stage OA SF licensed MSC(M), in the

presence or absence of IL-6 neutralizing antibody. Following 3 days of treatment, cells were washed with PBS, and phagocytosis of pHrodo™ Deep Red E. coli BioParticles® Conjugate (ThermoFisher Scientific, P35360) was assessed according to the manufacturer's protocol.

The particles were diluted 1:10 in 100 µL cell culture medium to achieve a final concentration of 10 µg/mL. Cells were incubated at 37°C for 1 hour, and fluorescence was measured using a plate reader with excitation and emission settings of 640 ± 15 nm and 690 ± 20 nm, respectively.

Proteome profiler array

The phosphorylation of protein kinases in $CD14^+$ monocytes treated with late-stage OA SF for 1 hour was assessed using the Human Phospho-Kinase Array Kit (R&D Systems; ARY003C), according to the manufacturer's instructions. The array detects phosphorylation at 37 kinase-specific sites. Signal intensities, representing the relative levels of phosphorylated proteins bound to each pair of duplicate spots, were quantified using ImageJ analysis software.

Statistical analysis

Statistical and graphical analyses were performed using Prism (GraphPad) and JMP Pro 18 (SAS). Normality tests were conducted prior to each analysis (significance level set at $p < 0.05$). In vitro data met normality tests. Parametric data from in vitro assays were analyzed using ordinary one-way ANOVA with Tukey's multiple comparisons test. For non-parametric data, including soluble factor concentrations and

immunophenotyping of MΦs in SF of OA patients, Kruskal-Wallis test with Dunn's multiple comparisons test was applied. A p-value of < 0.05 was considered statistically significant.

Supplemental material includes Fig. S1-S5 and Tables S1-S6.

Acknowledgements

This work is supported by the Arthritis Society (YIO-15-321) and CIHR (PJT-166089) to SV. The work is in part supported by the Schroeder Arthritis Institute via the Toronto General and Western Hospital Foundation (University Health Network). We thank the UHN Biobank, led by Mohit Kapoor and team, specifically Kim Perry, Christina Ward, and Luis Montoya from the Arthritis program, for their work in SF sample management, consent, and data collection. Dr. Vinod Chandran for providing psoriatic and rheumatoid arthritis SF samples. Schematics were developed using BioRender.com. Dr. R. Krawetz for providing non-OA cadaveric SF samples.

Author Contributions

Methodology, investigation, formal analysis and visualization, MR. Methodology, ABF. Writing original draft, formal analysis and visualization, KR. Visualization and editing, LR. Resources, RG. Conceptualization, writing, original draft and editing, supervision, project administration, fund acquisition, SV.

Declaration of interests

SV has 60% ownership of a regulatory consulting company, which does not conflict with the work done here. MR, ABF, RG, LR declare no conflicts. KR is currently employed by Stem Cell Technologies.

References

1. Steinmetz JD, Culbreth GT, Haile LM, Rafferty Q, Lo J, Fukutaki KG, et al. Global, regional, and national burden of osteoarthritis, 1990–2020 and projections to 2050: a systematic analysis for the Global Burden of Disease Study 2021. Lancet Rheumatol. 2023 Sept 1;5(9):e508–22.

2. Prieto-Potin I, Largo R, Roman-Blas JA, Herrero-Beaumont G, Walsh DA. Characterization of multinucleated giant cells in synovium and subchondral bone in knee osteoarthritis and rheumatoid arthritis. BMC Musculoskelet Disord. 2015 Aug 27;16:226.

3. Sowers M, Karvonen-Gutierrez CA, Jacobson JA, Jiang Y, Yosef M. Associations of Anatomical Measures from MRI with Radiographically Defined Knee Osteoarthritis Score, Pain, and Physical Functioning. JBJS. 2011 Feb 2;93(3):241.

4. Zhang Y, Nevitt M, Niu J, Lewis C, Torner J, Guermazi A, et al. Fluctuation of knee pain and changes in bone marrow lesions, effusions, and synovitis on magnetic resonance imaging. Arthritis Rheum. 2011 Mar;63(3):691–9.

5. Kraus VB, McDaniel G, Huebner JL, Stabler TV, Pieper CF, Shipes SW, et al. Direct in vivo evidence of activated macrophages in human osteoarthritis. Osteoarthritis Cartilage. 2016;24(9):1613–21.

6. Gómez-Aristizábal A, Gandhi R, Mahomed NN, Marshall KW, Viswanathan S. Synovial fluid monocyte/macrophage subsets and their correlation to patient-reported outcomes in osteoarthritic patients: a cohort study. Arthritis Res Ther. 2019 Jan 18;21(1):26.

7. Copp G, Robb KP, Viswanathan S. Culture-expanded mesenchymal stromal cell therapy: does it work in knee osteoarthritis? A pathway to clinical success. Cell Mol Immunol. 2023 June;20(6):626–50.

8. Najar M, Martel-Pelletier J, Pelletier JP, Fahmi H. Mesenchymal Stromal Cell Immunology for Efficient and Safe Treatment of Osteoarthritis. Front Cell Dev Biol. 2020 Sept 22;8:567813.

9. Hamilton AM, Cheung WY, Gómez-Aristizábal A, Sharma A, Nakamura S, Chaboureau A, et al. Iron nanoparticle-labeled murine mesenchymal stromal cells in an osteoarthritic model persists and suggests anti-inflammatory mechanism of action. PloS One. 2019;14(12):e0214107.

10. Chahal J, Gómez-Aristizábal A, Shestopaloff K, Bhatt S, Chaboureau A, Fazio A, et al. Bone Marrow Mesenchymal Stromal Cell Treatment in Patients with Osteoarthritis Results in Overall Improvement in Pain and Symptoms and Reduces Synovial Inflammation. Stem Cells Transl Med. 2019 Aug;8(8):746–57.

11. Gómez-Aristizábal A, Sharma A, Bakooshli MA, Kapoor M, Gilbert PM, Viswanathan S, et al. Stage-specific differences in secretory profile of mesenchymal stromal cells (MSCs) subjected to early- vs late-stage OA synovial fluid. Osteoarthritis Cartilage. 2017 May 1;25(5):737–41.

12. Kishimoto T, Kang S, Tanaka T. IL-6: A New Era for the Treatment of Autoimmune Inflammatory Diseases. In: Nakao K, Minato N, Uemoto S, editors. Innovative Medicine: Basic Research and Development [Internet]. Tokyo: Springer; 2015 [cited 2025 Jan 21]. Available from: http://www.ncbi.nlm.nih.gov/books/NBK500320/

13. Kim J, Hematti P. Mesenchymal stem cell–educated macrophages: A novel type of alternatively activated macrophages. Exp Hematol. 2009 Dec 1;37(12):1445–53.

14. Livshits G, Zhai G, Hart DJ, Kato BS, Wang H, Williams FMK, et al. Interleukin-6 is a significant predictor of radiographic knee osteoarthritis: The Chingford study. Arthritis Rheum. 2009 July;60(7):2037.

15. Relationships between Serum Interleukin-6, Radiographic Severity a WOMAC Index in Patients with Primary Knee Osteoarthritis. Egypt J Hosp Med. 2023 July 1;92(1):6082–6.

16. www.rndsystems.com [Internet]. [cited 2025 Sept 25]. Human IL-6 Antibody. Available from: https://www.rndsystems.com/products/human-il-6-antibody-1936_mab2061

17. Ii M, Sunamoto M, Uekata M, Sato J, Kitazaki T, Iizawa Y. TAK-242, a novel Toll-like receptor 4 signal transduction inhibitor, protects mice in Escherichia coli-induced and lipoteichoic acid-induced lethality models. Crit Care. 2006 Mar 21;10(1):P153.

18. Yan J, McCombe PA, Pender MP, Greer JM. Reduced IκB-α Protein Levels in Peripheral Blood Cells of Patients with Multiple Sclerosis—A Possible Cause of Constitutive NF-κB Activation. J Clin Med. 2020 Aug;9(8):2534.

19. Wang L, Walia B, Evans J, Gewirtz AT, Merlin D, Sitaraman SV. IL-6 Induces NF-κB Activation in the Intestinal Epithelia 1. J Immunol. 2003 Sept 15;171(6):3194–201.

20. Vogl T, Tenbrock K, Ludwig S, Leukert N, Ehrhardt C, van Zoelen MAD, et al. Mrp8 and Mrp14 are endogenous activators of Toll-like receptor 4, promoting lethal, endotoxin-induced shock. Nat Med. 2007 Sept;13(9):1042–9.

21. Li M, Wu ZM, Yang H, Huang SJ. NFκB and JNK/MAPK activation mediates the production of major macrophage- or dendritic cell-recruiting chemokine in human first trimester decidual cells in response to proinflammatory stimuli. J Clin Endocrinol Metab. 2011 Aug;96(8):2502–11.

22. Delprat V, Tellier C, Demazy C, Raes M, Feron O, Michiels C. Cycling hypoxia promotes a pro-inflammatory phenotype in macrophages via JNK/p65 signaling pathway. Sci Rep. 2020 Jan 21;10(1):882.

23. Han MS, Jung DY, Morel C, Lakhani SA, Kim JK, Flavell RA, et al. JNK Expression by Macrophages Promotes Obesity-induced Insulin Resistance and Inflammation. Science. 2012 Dec 6;339(6116):10.1126/science.1227568.

24. Yin Q, Song D, Chen J, Ning G, Wang W, Wang S. The CD14++CD16+ monocyte subset is expanded and controls Th1 cell development in Graves' disease. Clin Immunol. 2022 Dec 1;245:109160.

25. Rogacev KS, Cremers B, Zawada AM, Seiler S, Binder N, Ege P, et al. CD14++CD16+ Monocytes Independently Predict Cardiovascular Events: A Cohort Study of 951 Patients Referred for Elective Coronary Angiography. J Am Coll Cardiol. 2012 Oct 16;60(16):1512–20.

26. Metcalf TU, Wilkinson PA, Cameron MJ, Ghneim K, Chiang C, Wertheimer AM, et al. Human monocyte subsets are transcriptionally and functionally altered in aging in response to pattern recognition receptor agonists. J Immunol Baltim Md 1950. 2017 Aug 15;199(4):1405–17.

27. Shalova IN, Lim JY, Chittezhath M, Zinkernagel AS, Beasley F, Hernández-Jiménez E, et al. Human Monocytes Undergo Functional Re-programming during Sepsis Mediated by Hypoxia-Inducible Factor-1α. Immunity. 2015 Mar 17;42(3):484–98.

28. Mikulkova Z, Gallo J, Manukyan G, Trajerova M, Savara J, Shrestha B, et al. Complexity of synovial fluid-derived monocyte-macrophage-lineage cells in knee osteoarthritis. Cell Rep. 2024 Dec 24;43(12):115011.

29. Huang ZY, Stabler T, Pei FX, Kraus VB. Both systemic and local lipopolysaccharide (LPS) burden are associated with knee OA severity and inflammation. Osteoarthritis Cartilage. 2016 Oct;24(10):1769–75.

30. Özler K, Aktaş E, Atay Ç, Yılmaz B, Arıkan M, Güngör Ş. Serum and knee synovial fluid matrix metalloproteinase-13 and tumor necrosis factor-alpha levels in patients with late-stage osteoarthritis. Acta Orthop Traumatol Turc. 2016;50(3):356–61.

31. Gómez-Aristizábal A, Gandhi R, Mahomed NN, Marshall KW, Viswanathan S. Synovial fluid monocyte/macrophage subsets and their correlation to patient-reported outcomes in osteoarthritic patients: a cohort study. Arthritis Res Ther. 2019 Jan 18;21(1):26.

32. Mathiessen A, Conaghan PG. Synovitis in osteoarthritis: current understanding with therapeutic implications. Arthritis Res Ther. 2017 Feb 2;19(1):18.

33. Gobezie R, Kho A, Krastins B, Sarracino DA, Thornhill TS, Chase M, et al. High abundance synovial fluid proteome: distinct profiles in health and osteoarthritis. Arthritis Res Ther. 2007;9(2):R36.

34. Midwood K, Sacre S, Piccinini AM, Inglis J, Trebaul A, Chan E, et al. Tenascin-C is an endogenous activator of Toll-like receptor 4 that is essential for maintaining inflammation in arthritic joint disease. Nat Med. 2009 July;15(7):774–80.

35. Li L, Li Z, Li Y, Hu X, Zhang Y, Fan P. Profiling of inflammatory mediators in the synovial fluid related to pain in knee osteoarthritis. BMC Musculoskelet Disord. 2020 Feb 14;21(1):99.

36. Wiegertjes R, Loo FAJ van de, Davidson ENB. A roadmap to target interleukin-6 in osteoarthritis. Rheumatol Oxf Engl. 2020 July 21;59(10):2681.

37. de Hooge ASK, van de Loo FAJ, Bennink MB, Arntz OJ, de Hooge P, van den Berg WB. Male IL-6 gene knock out mice developed more advanced osteoarthritis upon aging. Osteoarthritis Cartilage. 2005 Jan;13(1):66–73.

38. Ryu JH, Yang S, Shin Y, Rhee J, Chun CH, Chun JS. Interleukin-6 plays an essential role in hypoxia-inducible factor 2α-induced experimental osteoarthritic cartilage destruction in mice. Arthritis Rheum. 2011 Sept;63(9):2732–43.

39. Kishimoto T, Akira S, Taga T. Interleukin-6 and its receptor: a paradigm for cytokines. Science. 1992 Oct 23;258(5082):593–7.

40. Babon JJ, Varghese LN, Nicola NA. Inhibition of IL-6 family cytokines by SOCS3. Semin Immunol. 2014 Feb;26(1):13–9.

41. Heinrich PC, Behrmann I, Haan S, Hermanns HM, Müller-Newen G, Schaper F. Principles of interleukin (IL)-6-type cytokine signalling and its regulation. Biochem J. 2003 Aug 15;374(Pt 1):1–20.

42. Hibi M, Murakami M, Saito M, Hirano T, Taga T, Kishimoto T. Molecular cloning and expression of an IL-6 signal transducer, gp130. Cell. 1990 Dec 21;63(6):1149–57.

43. Wu X, Cao L, Li F, Ma C, Liu G, Wang Q. Interleukin-6 from subchondral bone mesenchymal stem cells contributes to the pathological phenotypes of experimental osteoarthritis. Am J Transl Res. 2018;10(4):1143–54.

44. Rose-John S. The Soluble Interleukin 6 Receptor: Advanced Therapeutic Options in Inflammation. Clin Pharmacol Ther. 2017;102(4):591–8.

45. Lust JA, Donovan KA, Kline MP, Greipp PR, Kyle RA, Maihle NJ. Isolation of an mRNA encoding a soluble form of the human interleukin-6 receptor. Cytokine. 1992 Mar;4(2):96–100.

46. Riethmueller S, Somasundaram P, Ehlers JC, Hung CW, Flynn CM, Lokau J, et al. Proteolytic Origin of the Soluble Human IL-6R In Vivo and a Decisive Role of N-Glycosylation. PLoS Biol. 2017 Jan;15(1).

47. Rose-John S, Heinrich PC. Soluble receptors for cytokines and growth factors: generation and biological function. Biochem J. 1994 June 1;300(2):281–90.

48. Reeh H, Rudolph N, Billing U, Christen H, Streif S, Bullinger E, et al. Response to IL-6 trans- and IL-6 classic signalling is determined by the ratio of the IL-6 receptor α to gp130 expression: fusing experimental insights and dynamic modelling. Cell Commun Signal CCS. 2019 May 17;17:46.

49. Bauer J, Bauer TM, Kalb T, Taga T, Lengyel G, Hirano T, et al. Regulation of interleukin 6 receptor expression in human monocytes and monocyte-derived macrophages. Comparison with the expression in human hepatocytes. J Exp Med. 1989 Nov 1;170(5):1537–49.

50. Yasukawa H, Ohishi M, Mori H, Murakami M, Chinen T, Aki D, et al. IL-6 induces an anti-inflammatory response in the absence of SOCS3 in macrophages. Nat Immunol. 2003 June;4(6):551–6.

51. Karin M, Ben-Neriah Y. Phosphorylation meets ubiquitination: the control of NF-[kappa]B activity. Annu Rev Immunol. 2000;18:621–63.

52. Chen WC, Wang SW, Lin CY, Tsai CH, Fong YC, Lin TY, et al. Resistin Enhances Monocyte Chemoattractant Protein-1 Production in Human Synovial Fibroblasts and Facilitates Monocyte Migration | Cell Physiol Biochem. Cell Physiol Biochem. 2019 Mar 8;52(3):408–20.

53. Wei X, Yi X, Liu J, Sui X, Li L, Li M, et al. Circ-phkb promotes cell apoptosis and inflammation in LPS-induced alveolar macrophages via the TLR4/MyD88/NF-kB/CCL2 axis. Respir Res. 2024 Jan 29;25(1):62.

54. Russo A, Schürmann H, Brandt M, Scholz K, Matos ALL, Grill D, et al. Alarming and Calming: Opposing Roles of S100A8/S100A9 Dimers and Tetramers on Monocytes. Adv Sci. 2022 Oct 30;9(36):2201505.

55. Lv H, Liu Q, Sun Y, Yi X, Wei X, Liu W, et al. Mesenchymal stromal cells ameliorate acute lung injury induced by LPS mainly through stanniocalcin-2 mediating macrophage polarization. Ann Transl Med. 2020 Mar;8(6):334–334.

56. Galleu A, Riffo-Vasquez Y, Trento C, Lomas C, Dolcetti L, Cheung TS, et al. Apoptosis in mesenchymal stromal cells induces in vivo recipient-mediated immunomodulation. Sci Transl Med. 2017 Nov 15;9(416):eaam7828.

57. Kim YE, Sung DK, Bang Y, Sung SI, Yang M, Ahn SY, et al. SOCS3 Protein Mediates the Therapeutic Efficacy of Mesenchymal Stem Cells against Acute Lung Injury. Int J Mol Sci. 2023 May 4;24(9):8256.

58. Bouffi C, Bony C, Courties G, Jorgensen C, Noël D. IL-6-dependent PGE2 secretion by mesenchymal stem cells inhibits local inflammation in experimental arthritis. PloS One. 2010 Dec 7;5(12):e14247.

59. Prockop DJ. Inflammation, fibrosis, and modulation of the process by mesenchymal stem/stromal cells. Matrix Biol J Int Soc Matrix Biol. 2016 Apr;51:7–13.

60. Mittal M, Tiruppathi C, Nepal S, Zhao YY, Grzych D, Soni D, et al. TNFα-stimulated gene-6 (TSG6) activates macrophage phenotype transition to prevent inflammatory lung injury. Proc Natl Acad Sci. 2016 Dec 13;113(50):E8151–8.

61. Zhang C, Zhang B, Wang H, Tao Q, Ge S, Zhai Z. Tumor necrosis factor alpha-stimulated gene-6 (TSG-6) inhibits the inflammatory response by inhibiting the activation of P38 and JNK signaling pathway and decreases the restenosis of vein grafts in rats. Heart Vessels. 2017 Dec;32(12):1536–45.

62. Amin AR, Attur M, Patel RN, Thakker GD, Marshall PJ, Rediske J, et al. Superinduction of cyclooxygenase-2 activity in human osteoarthritis-affected cartilage. Influence of nitric oxide. J Clin Invest. 1997 Mar 15;99(6):1231–7.

63. Li X, Ellman M, Muddasani P, Wang JHC, Cs-Szabo G, van Wijnen AJ, et al. PGE2 And Its Cognate EP Receptors Control Human Adult Articular Cartilage Homeostasis and Are Linked to the Pathophysiology of Osteoarthritis. Arthritis Rheum. 2009 Feb;60(2):513–23.

64. Maekawa A, Sawaji Y, Endo K, Kusakabe T, Konishi T, Tateiwa T, et al. Prostaglandin E2 induces dual-specificity phosphatase-1, thereby attenuating inflammatory genes expression in human osteoarthritic synovial fibroblasts. Prostaglandins Other Lipid Mediat. 2021 June 1;154:106550.

65. Del Sordo L, Blackler GB, Philpott HT, Riviere J, Gunaratnam L, Heit B, et al. Impaired Efferocytosis by Synovial Macrophages in Patients With Knee Osteoarthritis. Arthritis Rheumatol Hoboken NJ. 2023 May;75(5):685–96.

66. Huber R, Bikker R, Welz B, Christmann M, Brand K. TNF Tolerance in Monocytes and Macrophages: Characteristics and Molecular Mechanisms. J Immunol Res. 2017;2017:9570129.

67. Roos EM, Roos HP, Lohmander LS, Ekdahl C, Beynnon BD. ePROVIDE - Mapi Research Trust. 1998. Knee injury and Osteoarthritis Outcome Score (KOOS).

Available from: https://eprovide.mapi-trust.org/instruments/knee-injury-and-osteoarthritis-outcome-score

68. George S, Georgouli M, Sanz-Moreno V. Protocol to drive human monocyte-to-macrophage polarization *in vitro* using tumor conditioned media. STAR Protoc. 2022 Dec 16;3(4):101666.

69. Gómez-Aristizábal A, Kim KP, Viswanathan S. A Systematic Study of the Effect of Different Molecular Weights of Hyaluronic Acid on Mesenchymal Stromal Cell-Mediated Immunomodulation. PLOS ONE. 2016 Jan 28;11(1):e0147868.

70. Waise TMZ, Rasti M, Duca FA, Zhang SY, Bauer PV, Rhodes CJ, et al. Inhibition of upper small intestinal mTOR lowers plasma glucose levels by inhibiting glucose production. Nat Commun. 2019 Feb 12;10(1):714.

Figure legends

Figure 1. OA synovial fluid contains different cytokines, chemokines and MΦ subsets displaying mixed phenotypes

(A-D) Median and interquartile range of IL-6, chemokine (C-C motif) ligand 2 (CCL2), S100A8/9, and IL-8 concentrations in synovial fluid (SF) samples from not OA SF (Not OA; N=6-11); mid-stage OA SF (Mid OA; N=21-30); late-stage OA SF (Late-OA; N=29-35). **(E)** Frequency of MΦ subsets in the late-OA SF. **(F-I)** The mean fluorescence intensity (MFI) expression of CD163, CD206, HLA-DR, and HLA-DR/CD163 MFI expression ratio, in late-OA SF MΦ subsets (N=25-43). **(J)** Immunophenotyping, intracellular IL-1β and TNF evaluation of late-OA SF MΦ following re-challenge with lipopolysaccharides (LPS, 10 ng/mL; N=4). Kruskal-Wallis test with Dunn's multiple comparisons test was used (*$p<0.05$; ** $p< 0.001$; ***$p<0.0001$; **** $p< 0.00001$).

Figure 2. Exposure of peripheral CD14$^+$ monocytes to late-OA SF partially increased the frequency of the intermediate monocyte subset and partially tolerized them

(A) Frequency of classical (CD14$^+$CD16^{neg}) and intermediate (CD14$^+$CD16$^+$) peripheral healthy CD14$^+$ monocyte subsets with and without OA synovial fluid (SF). **(B, C)** Mean fluorescence intensity (MFI) of CD163, CD206, HLA-DR, and CD86 surface markers, and HLA-DR/CD163 MFI ratio on (●) healthy and (□) OA peripheral CD14$^+$ monocytes and tumor necrosis factor (TNF) production, with or without late-stage OA SF, following lipopolysaccharide (LPS, 2.5 ng/mL) re-challenge. **(D)** Percent intermediate (CD14$^+$CD16$^+$) monocytes in healthy CD45$^+$ cells with indicated treatments. **(E-I)** MFI expression of CD163, CD206, HLA-DR, and CD86 cell surface markers and HLA-DR/CD163 MFI expression ratio on healthy peripheral CD14$^+$ monocytes at the indicated conditions. **(J)** TNF soluble factor production by healthy peripheral CD14$^+$ monocytes in indicated treatments, normalized relative to control LPS (2.5 ng/mL) stimulation. Peripheral CD14$^+$ monocytes were cultured for 72h with indicated treatments in (A-I) for flow cytometry assay and 48 hours in (B and J) for TNF assay; IL-6 recombinant (5 ng/mL); IL-6 neutralizing antibody (Ab; 2.5 µg/mL); 30% pooled mid- or late-OA SF. Values are shown as mean ± SD; N=3 biological replicates; n $\geq$ 3 technical replicates. An ordinary one-way ANOVA with Tukey's multiple comparisons test was used. Letters indicate significant differences ($p < 0.05$) between groups; asterisks indicate significance ($p<0.05$) relative to untreated or LPS-treated controls.

Figure 3. Physiological levels of IL-6 in OA SF signal through classical, not trans-signaling

(A) Schematic representation of dual IL-6 signaling in cells such as monocytes/macrophages (MΦs) expressing IL-6 receptor (IL-6R): i) trans-signaling through glycoprotein (gp)130 and soluble IL-6R (sIL-6R shed by a disintegrin and metalloproteinase 17 (ADAM 17)); ii) classical signaling through membrane-bound (m) IL-6R and gp130. **(B)** Median and interquartile range of sIL-6R concentration in synovial fluid (SF) samples from not-OA (N=7); mid-OA (N=24); and late-OA (N=43). **(C-F)** Mean fluorescence intensity (MFI) expression of CD163, CD206, HLA-DR and CD86 surface markers in the presence of late-OA SF and physiological levels of IL-6 (0.5 ng/mL) or/and sIL-6R (10 ng/mL), soluble(s) gp130 (10 ng/mL) in healthy donors. **(G)** mIL-6R expression on healthy $CD14^+$ monocytes at the indicated treatments. **(H)** IL-6: sIL-6R complex levels in not-OA SF (N=7); mid-OA SF (N=24); late-OA SF (N=72), psoriatic arthritis (PsA) SF (N=2) and rheumatoid arthritis (RA) SF (N=1). Healthy peripheral $CD14^+$ monocytes were cultured for 72h with 30% pooled mid- or late-OA SFs, IL-6 neutralizing antibody (Ab; 2.5 µg/mL), and indicated treatments. MFI expression of monocyte cell surface markers is shown as mean ± SD; N=3 biological replicates; n=3 technical replicates. An ordinary one-way ANOVA with Tukey's multiple comparisons test was used. Letters indicate significant differences ($p < 0.05$) between groups; asterisks indicate significance ($p<0.05$) relative to untreated controls.

Figure 4. Late-OA SF stimulated multiple signaling pathways in $CD14^+$ monocytes, partially replicated by IL-6 and S100A8/9 stimulation

(A) An experimental timeline for healthy CD14 monocytes indicating treatment conditions at each time point (arrows) for both short- and long-term exposure periods. **(B)** Representative western blot images from healthy $CD14^+$ monocytes at short treatment exposures. **(C)** Representative western blot images from healthy $CD14^+$ monocytes at long treatment exposures. **(D-F)** Bar graphs illustrating phosphorylated-signal transducer and activator of transcription 3 (p-STAT3), phosphorylated-c-Jun terminal kinase (p-JNK), and nuclear factor of kappa light polypeptide gene enhancer in B-cells inhibitor alpha (IκBα) levels (normalized to total glyceraldehyde-3-phosphate dehydrogenase; GAPDH) in short and long treatment exposures. **(G)** Suppressor of cytokine signaling 3 (SOCS3) expression in healthy $CD14^+$ monocytes with indicated treatments. **(H)** Chemokine (C-C motif) ligand 2 (CCL2) expression in healthy $CD14^+$ monocytes with indicated treatments. **(I)** Tumor necrosis factor (TNF) expression by healthy $CD14^+$ monocytes in indicated treatments with LPS (2.5 ng/mL) stimulation. Healthy peripheral $CD14^+$ monocytes were cultured for 48h (G-I); IL-6 recombinant (5 ng/mL); S100A8/9 recombinant (1 µg/mL); IL-6 neutralizing antibody (Ab; 2.5 µg/mL); 30% pooled late-OA synovial fluid (SF); TAK242 (1 µM/mL). Values are shown as mean ± SD; N=3 biological replicates; n≤3 technical replicates. An ordinary one-way ANOVA with Tukey's multiple comparisons test was used. Letters indicate significant differences ($p< 0.05$) between groups; asterisks indicate significance ($p<0.05$) relative to untreated controls.

Figure 5. Direct co-culture of MSC(M) with $CD14^+$ monocytes further immunosuppressed them even in late-OA SF

(A) Experimental timeline and schematic workflow for healthy and OA $CD14^+$ monocytes directly co-cultured with MSC(M); 30% pooled mid- or late-OA synovial fluid (SF) or IL-6 neutralizing antibody (Ab; 2.5 µg/mL) for 72h. (**B, C)** Mean fluorescence intensity (MFI) of CD163, CD206, HLA-DR, and CD86 surface markers, and HLA-DR/CD163 MFI ratio on (●) healthy and (□) OA peripheral $CD14^+$ monocytes directly co-cultured with MSC(M), with or without late-stage OA SF. **(D-H)** MFI expression of CD163, CD206, HLA-DR, CD86 cell surface markers and the ratio of HLA-DR/CD163 MFI expression on healthy $CD14^+$ monocytes directly co-cultured with MSC(M) at indicated treatments. Values are shown as mean ± SD; N=3 biological replicates; n≤3 technical replicates. An ordinary one-way ANOVA with Tukey's multiple comparisons test was used. Letters indicate significant differences ($p<0.05$) between groups; asterisks indicate significance ($p<0.05$) relative to untreated controls.

Figure 6. Soluble factors from licensed MSC(M) CM in late-stage OA SF attenuated pro-inflammatory signaling kinases, functionality, and activated downstream effector genes in $CD14^+$ monocytes

(A) Experimental timeline and schematic workflow for secondary healthy and OA $CD14^+$ monocytes treated with soluble factors from licensed MSC(M) CM in OA environment. **(B, C)** Representative western blot images of healthy and OA $CD14^+$ monocytes. **(D)** phosphorylated-signal transducer and activator of transcription 3 (p-STAT3), phosphorylated-c-Jun terminal kinase (p-JNK), and nuclear factor of kappa light polypeptide gene enhancer in B-cells inhibitor alpha (IκBα) levels (normalized to total glyceraldehyde-3-phosphate dehydrogenase; GAPDH) and normalized TNF production

(relative to LPS alone controls) in (●) healthy and (□) OA $CD14^+$ monocytes. **(E-F)** Bar graphs illustrating p-STAT3, p-JNK, and IκBα levels (normalized to total GAPDH) at indicated treatments in healthy $CD14^+$ monocytes. **(H)** Expression of the suppressor of cytokine signaling 3 (SOCS3*)* gene in treated healthy $CD14^+$ monocytes. **(I and J)** JNK downstream chemokine (C-C motif) ligand 2 (CCL2*)* and tumor necrosis factor (TNF*)* genes expression in treated healthy $CD14^+$ monocytes. **(K)** Normalized TNF soluble factor production by healthy peripheral $CD14^+$ monocytes in indicated treatments to LPS (2.5 ng/mL) stimulation. **(L)** Phagocytosis of pHrodo Deep Red E. coli BioParticles by healthy macrophages in indicated treatments for 72h. Peripheral $CD14^+$ monocytes were treated with CM of directly co-cultured monocytes with MSC(M), and mid- or late-OA SF ± IL-6 neutralizing antibody (Ab, 2.5 µg/mL); 30% pooled mid- or late synovial fluid (SF). Gene expression in (H-J) and TNF soluble in (D, K) were assessed after 48h. Values are shown as mean ± SD; N=3 biological replicates; n ≥ 3 technical replicates. An ordinary one-way ANOVA with Tukey's multiple comparisons test was used. Different letters indicate significant differences ($p < 0.05$) between groups; asterisks indicate significance ($p<0.05$) relative to untreated controls.

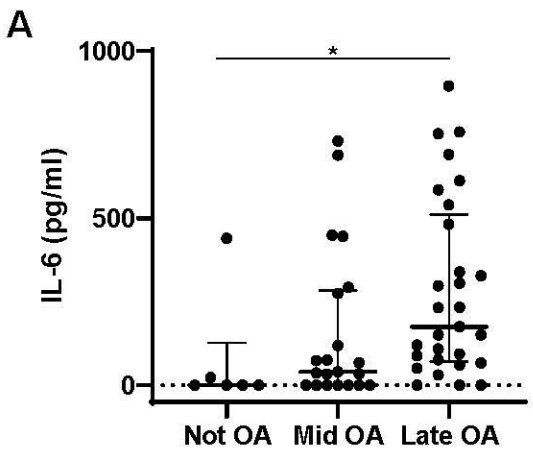

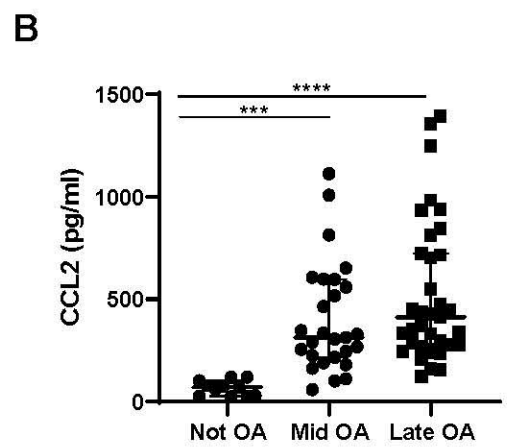

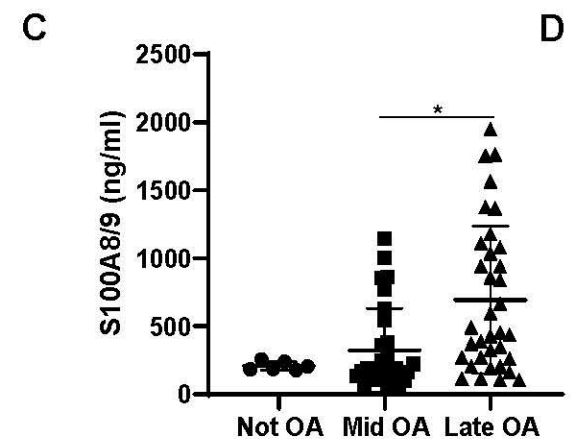

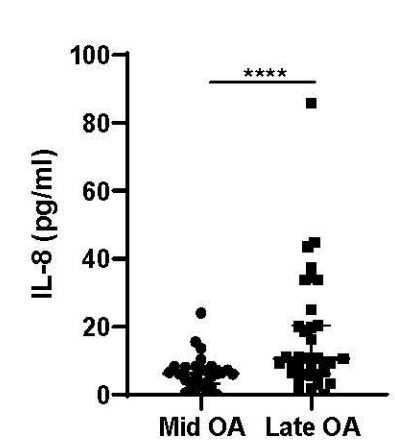

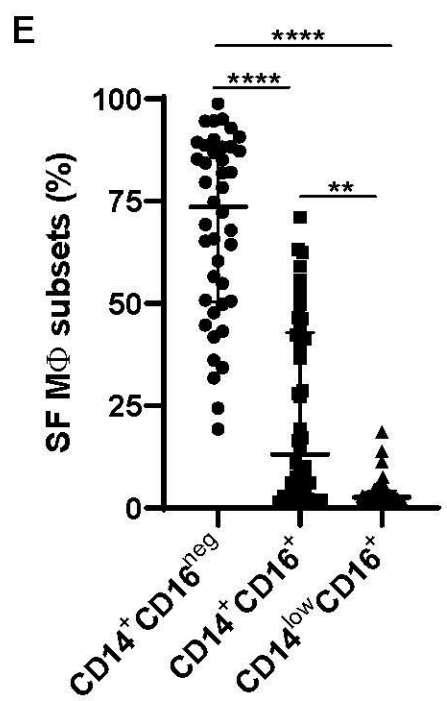

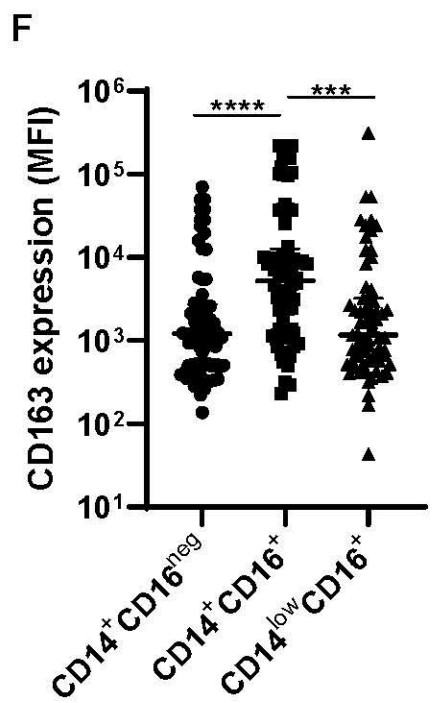

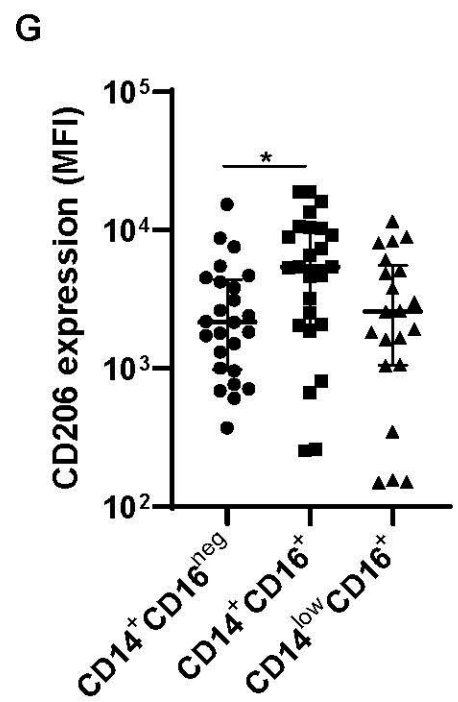

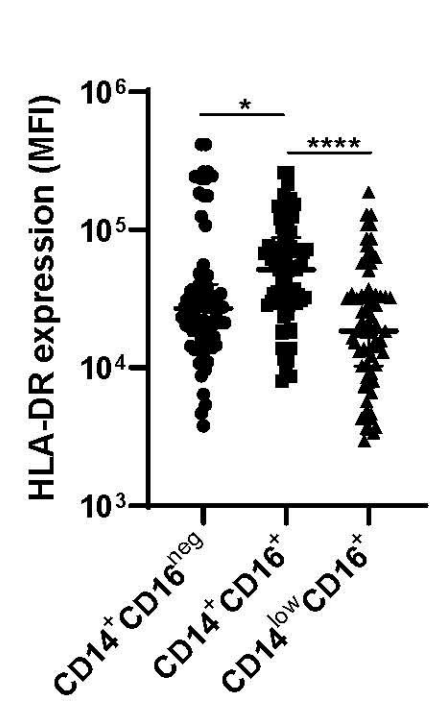

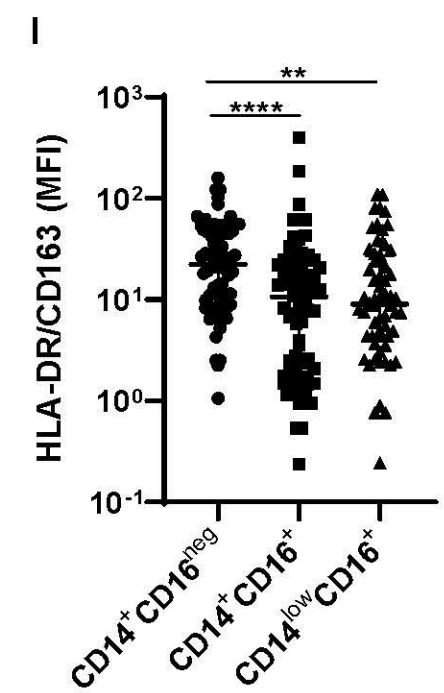

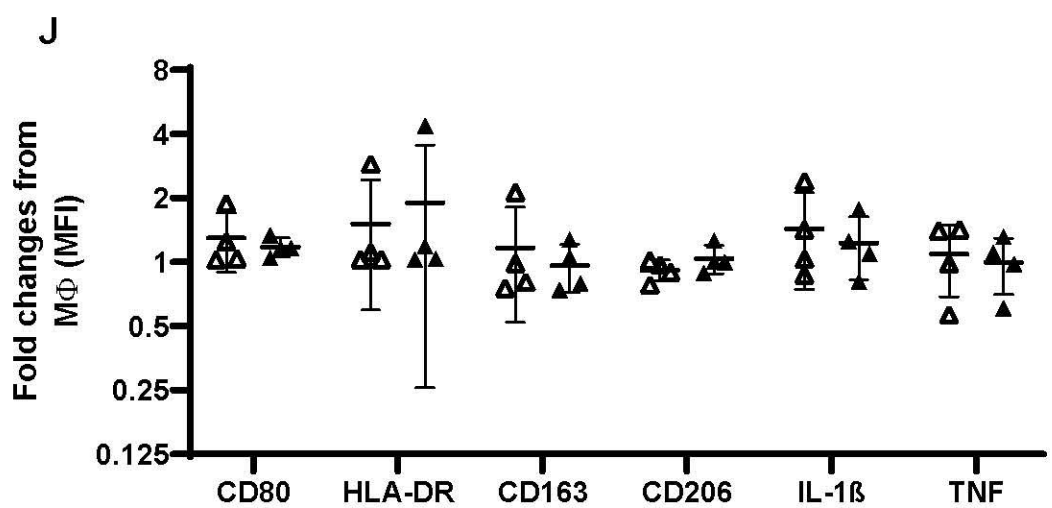

+ LPS 4h

+ LPS 48h+4h

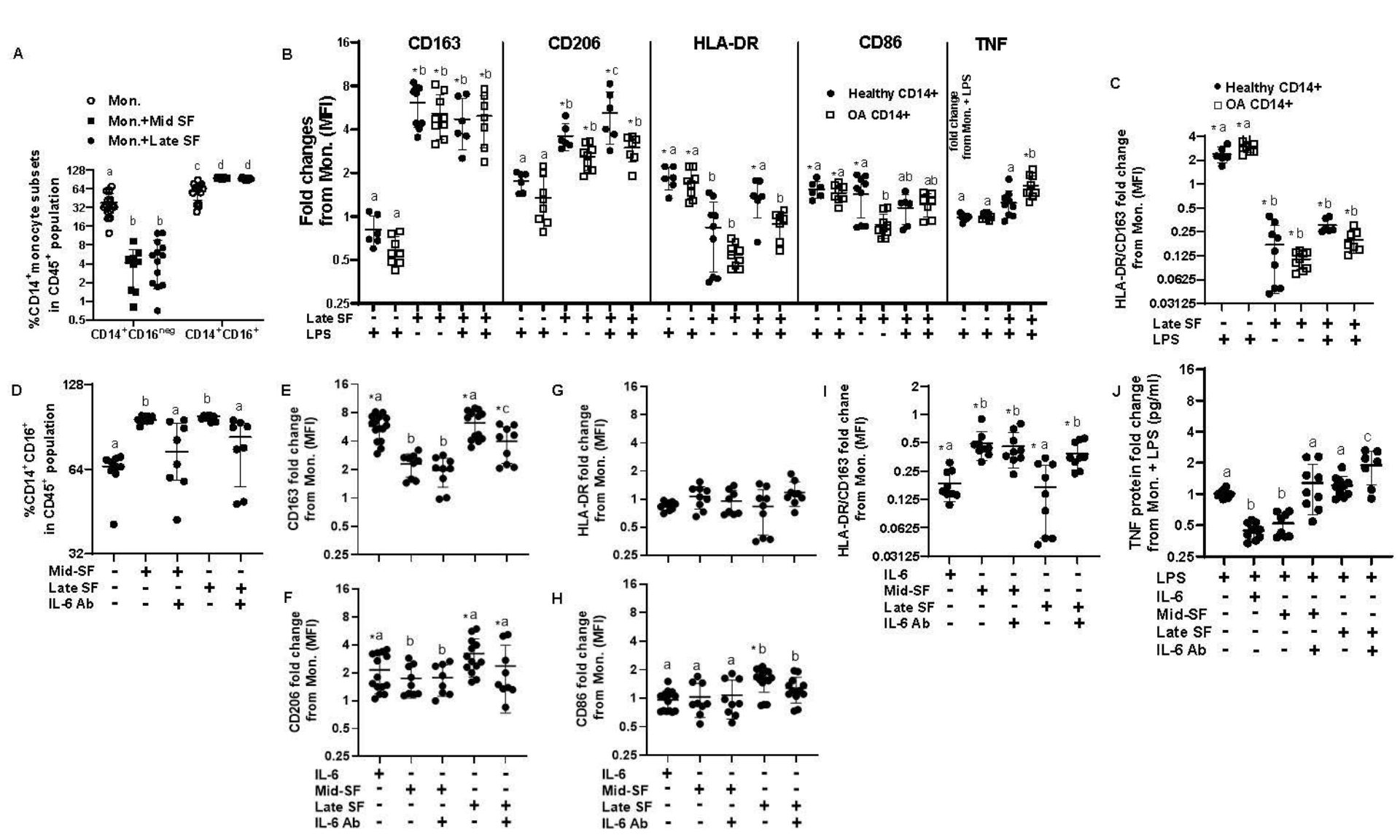
A
Mon.
Mon.+Mid SF
Mon.+Late SF
%CD14+monocyte subsets in CD45+ population
CD14+CD16neg
CD14+CD16+
B
CD163
CD206
HLA-DR
CD86
TNF
Fold changes from Mon. (MFI)
Healthy CD14+
OA CD14+
fold change from Mon. + LPS
Late SF
LPS
C
Healthy CD14+
OA CD14+
HLA-DR/CD163 fold change from Mon. (MFI)
Late SF
LPS
D
%CD14+CD16+ in CD45+ population
Mid-SF
Late SF
IL-6 Ab
E
CD163 fold change from Mon. (MFI)
F
CD206 fold change from Mon. (MFI)
IL-6
Mid-SF
Late SF
IL-6 Ab
G
HLA-DR fold change from Mon. (MFI)
H
CD86 fold change from Mon. (MFI)
IL-6
Mid-SF
Late SF
IL-6 Ab
I
HLA-DR/CD163 fold chane from Mon. (MFI)
IL-6
Mid-SF
Late SF
IL-6 Ab
J
TNF protein fold change from Mon. + LPS (pg/ml)
LPS
IL-6
Mid-SF
Late SF
IL-6 Ab

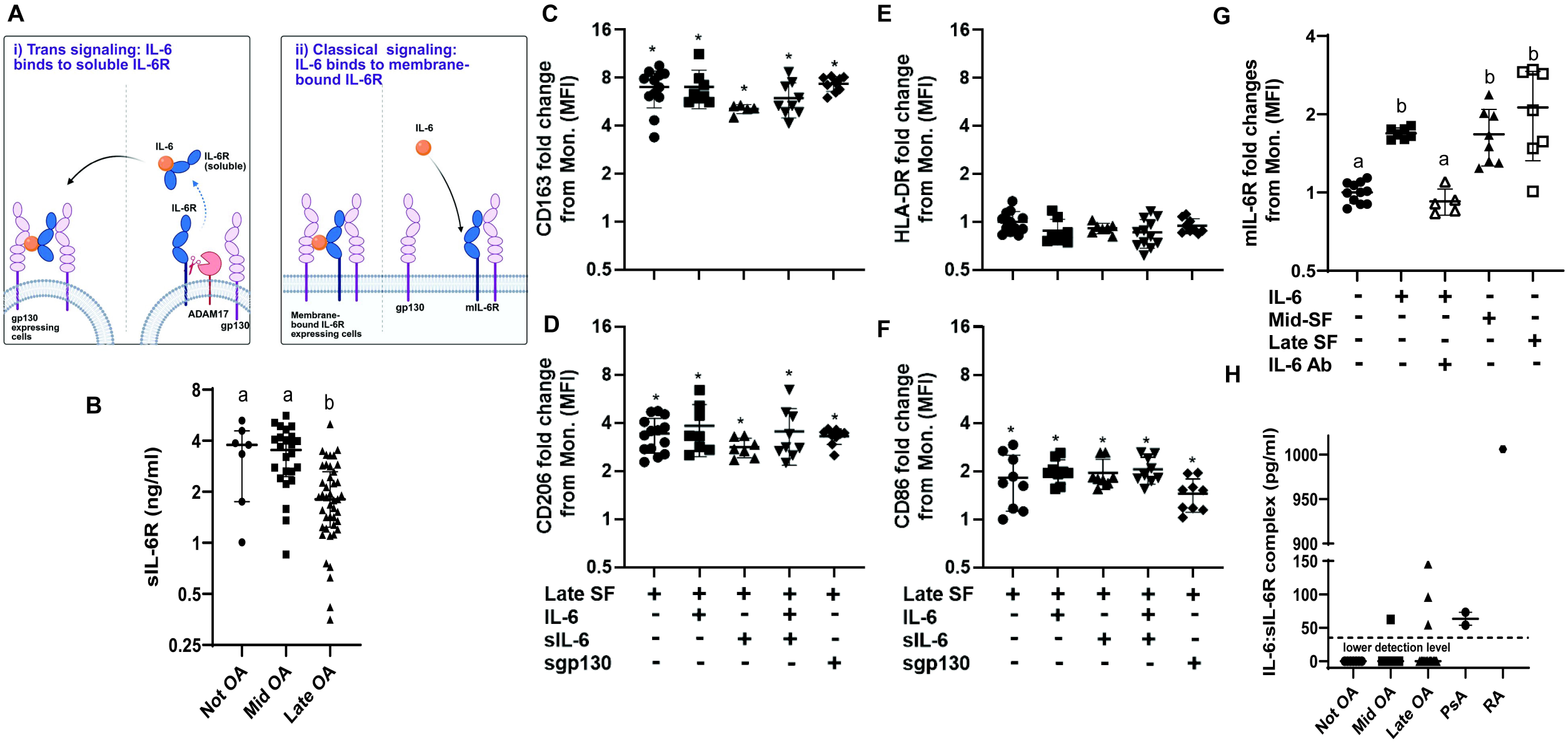
A
i) Trans signaling: IL-6 binds to soluble IL-6R
IL-6
IL-6R (soluble)
IL-6R
ADAM17
gp130
gp130 expressing cells
ii) Classical signaling: IL-6 binds to membrane-bound IL-6R
IL-6
gp130
mIL-6R
Membrane-bound IL-6R expressing cells
B
sIL-6R (ng/ml)
Not OA
Mid OA
Late OA
C
CD163 fold change from Mon. (MFI)
D
CD206 fold change from Mon. (MFI)
Late SF
IL-6
sIL-6
sgp130
E
HLA-DR fold change from Mon. (MFI)
F
CD86 fold change from Mon. (MFI)
G
mIL-6R fold changes from Mon. (MFI)
IL-6
Mid-SF
Late SF
IL-6 Ab
H
IL-6:sIL-6R complex (pg/ml)
lower detection level
Not OA
Mid OA
Late OA
PsA
RA

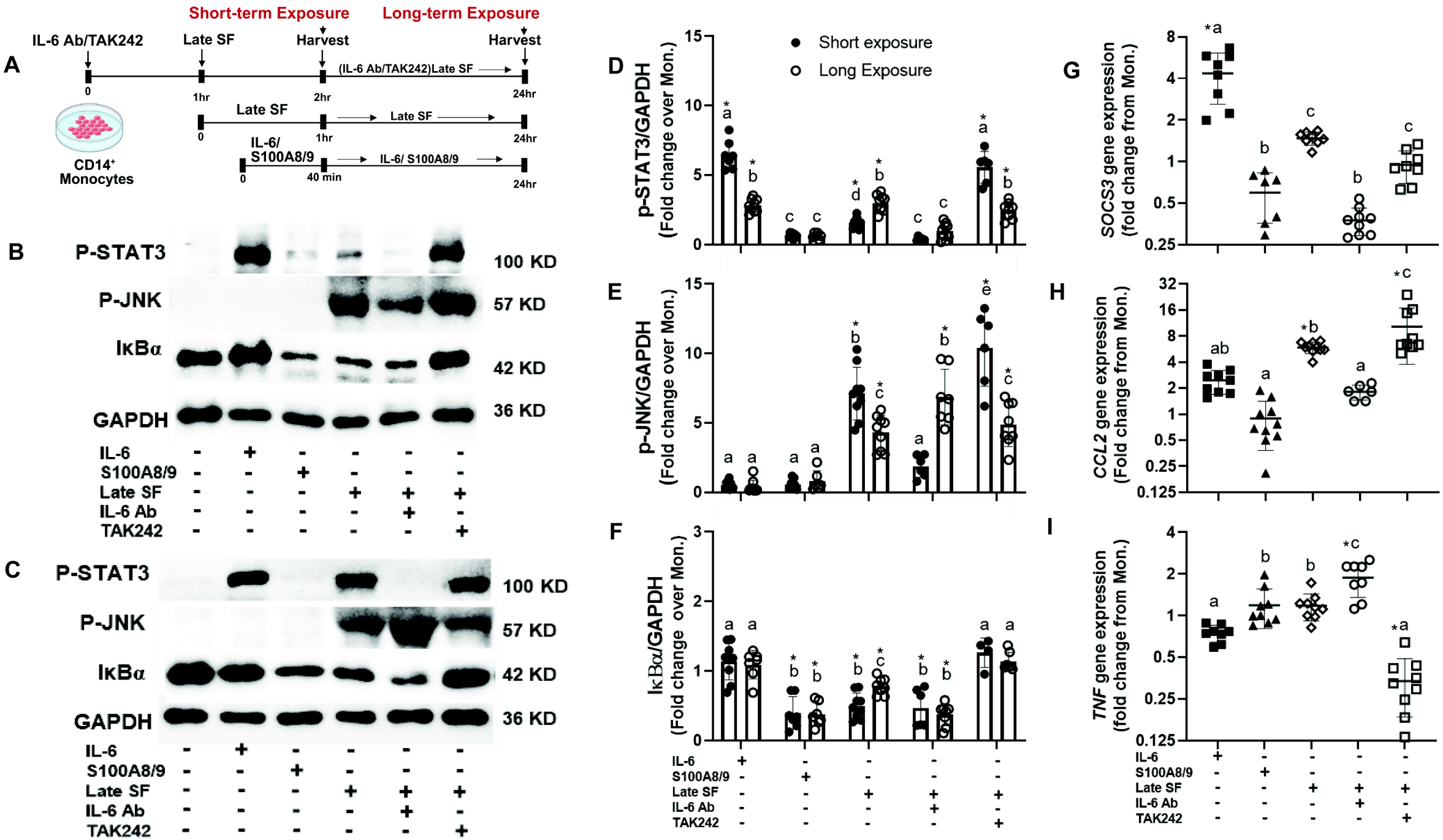
A
Short-term Exposure
Long-term Exposure
IL-6 Ab/TAK242
Late SF
Harvest
Harvest
(IL-6 Ab/TAK242)Late SF
0
1hr
2hr
24hr
Late SF
Late SF
0
1hr
24hr
IL-6/
S100A8/9
IL-6/ S100A8/9
0
40 min
24hr
CD14+
Monocytes
B
P-STAT3
P-JNK
IκBα
GAPDH
100 KD
57 KD
42 KD
36 KD
IL-6
S100A8/9
Late SF
IL-6 Ab
TAK242
C
P-STAT3
P-JNK
IκBα
GAPDH
100 KD
57 KD
42 KD
36 KD
IL-6
S100A8/9
Late SF
IL-6 Ab
TAK242
D
Short exposure
Long Exposure
p-STAT3/GAPDH
(Fold change over Mon.)
E
p-JNK/GAPDH
(Fold change over Mon.)
F
IκBα/GAPDH
(Fold change over Mon.)
IL-6
S100A8/9
Late SF
IL-6 Ab
TAK242
G
SOCS3 gene expression
(fold change from Mon.)
H
CCL2 gene expression
(Fold change from Mon.)
I
TNF gene expression
(fold change from Mon.)
IL-6
S100A8/9
Late SF
IL-6 Ab
TAK242

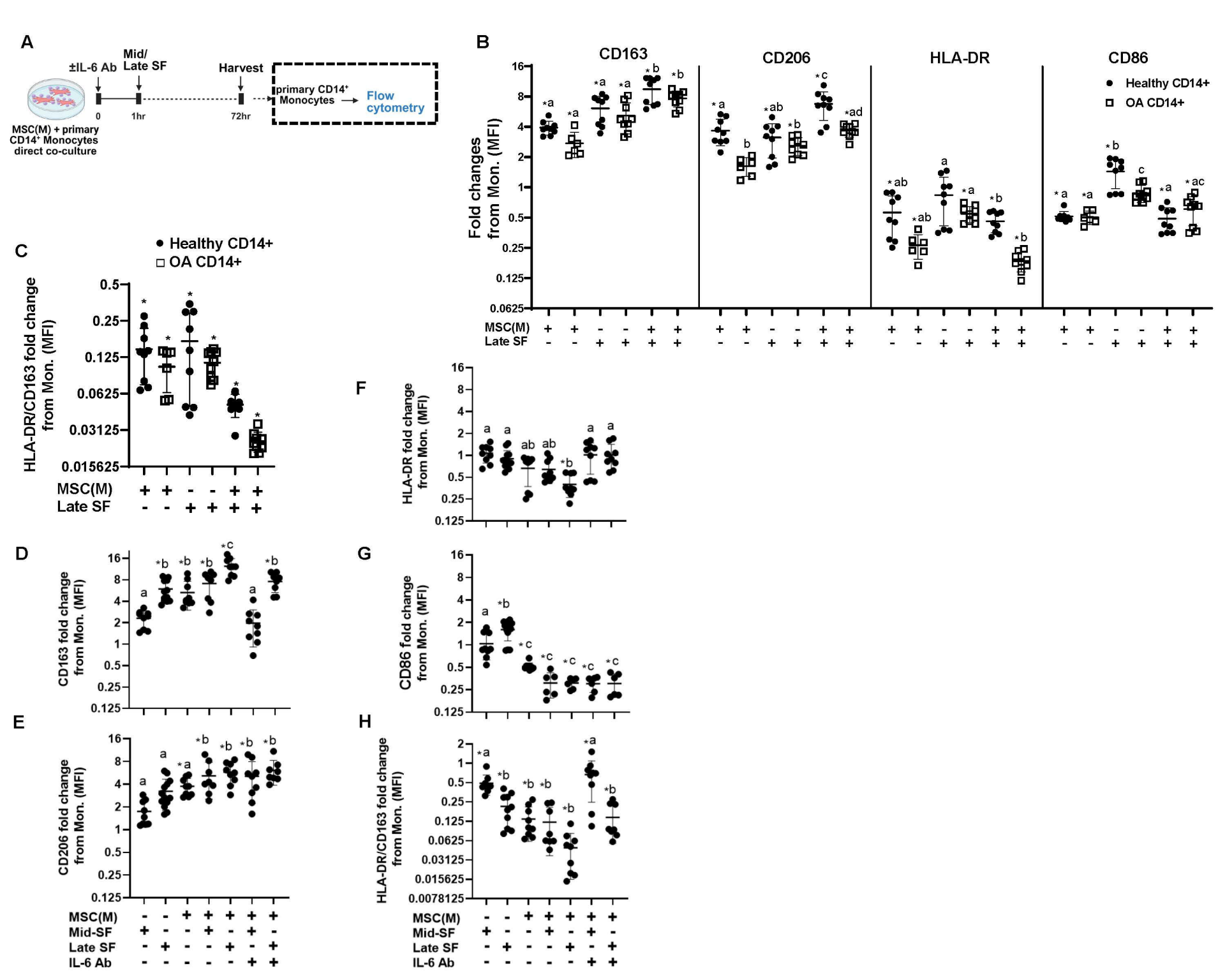
A
±IL-6 Ab
Mid/
Late SF
Harvest
0
1hr
72hr
MSC(M) + primary
CD14+ Monocytes
direct co-culture
primary CD14+
Monocytes
Flow
cytometry
B
CD163
CD206
HLA-DR
CD86
Healthy CD14+
OA CD14+
Fold changes
from Mon. (MFI)
MSC(M)
Late SF
C
Healthy CD14+
OA CD14+
HLA-DR/CD163 fold change
from Mon. (MFI)
MSC(M)
Late SF
D
CD163 fold change
from Mon. (MFI)
E
CD206 fold change
from Mon. (MFI)
MSC(M)
Mid-SF
Late SF
IL-6 Ab
F
HLA-DR fold change
from Mon. (MFI)
G
CD86 fold change
from Mon. (MFI)
H
HLA-DR/CD163 fold change
from Mon. (MFI)
MSC(M)
Mid-SF
Late SF
IL-6 Ab

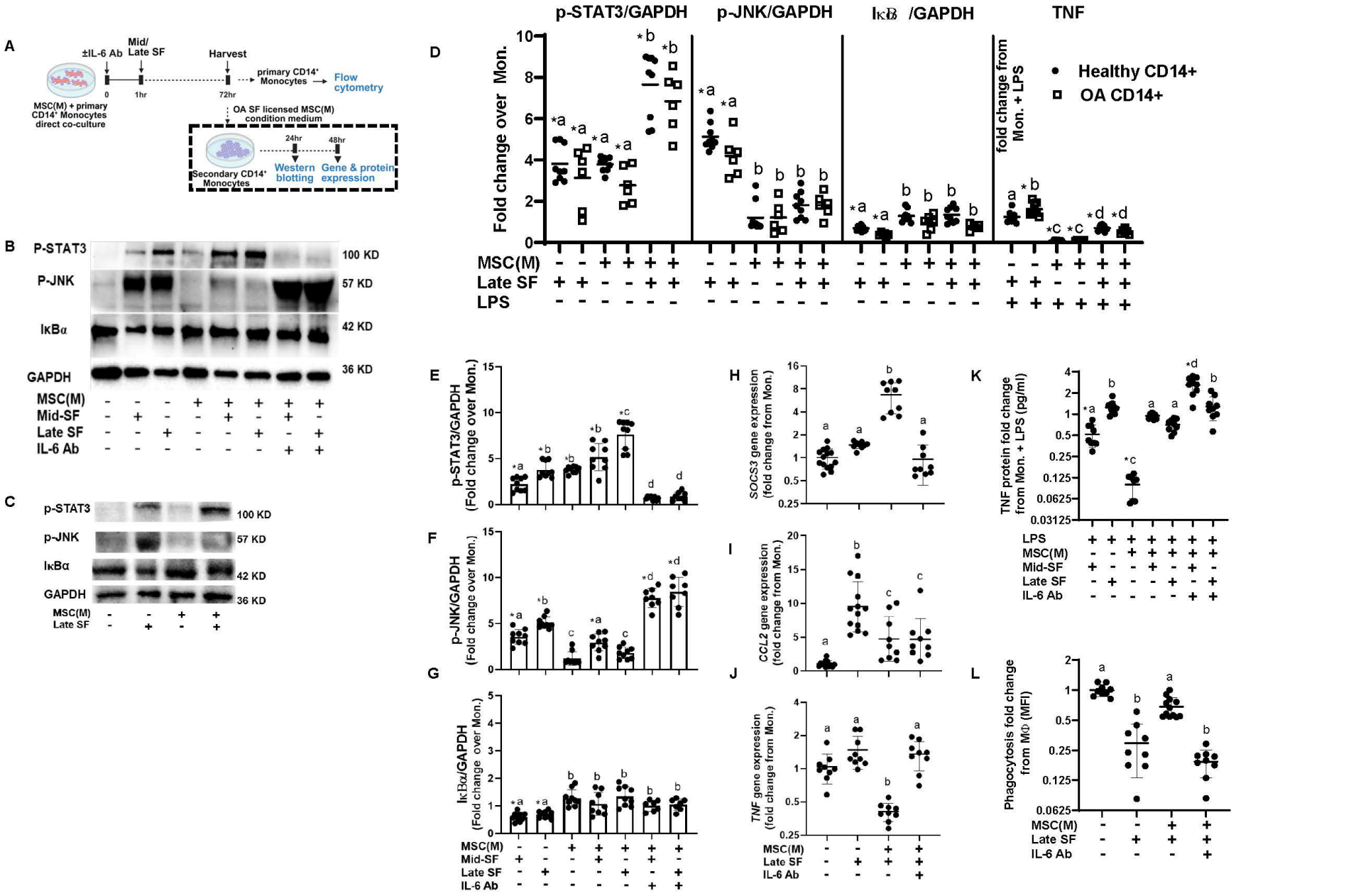
A
±IL-6 Ab
Mid/ Late SF
Harvest
primary CD14+ Monocytes
Flow cytometry
MSC(M) + primary CD14+ Monocytes direct co-culture
OA SF licensed MSC(M) condition medium
Secondary CD14+ Monocytes
Western blotting
Gene & protein expression
B
P-STAT3
P-JNK
IκBα
GAPDH
100 KD
57 KD
42 KD
36 KD
MSC(M)
Mid-SF
Late SF
IL-6 Ab
C
D
p-STAT3/GAPDH
p-JNK/GAPDH
IκB /GAPDH
TNF
Fold change over Mon.
fold change from Mon. + LPS
Healthy CD14+
OA CD14+
LPS
E
p-STAT3/GAPDH (Fold change over Mon.)
F
p-JNK/GAPDH (Fold change over Mon.)
G
IκBα/GAPDH (Fold change over Mon.)
H
SOCS3 gene expression (fold change from Mon.)
I
CCL2 gene expression (fold change from Mon.)
J
TNF gene expression (fold change from Mon.)
K
TNF protein fold change from Mon. + LPS (pg/ml)
L
Phagocytosis fold change from MΦ (MFI)